This is article has been published in the *Journal of Occupational and Environmental Hygiene* and is available online at: https://doi.org/10.1080/15459624.2019.1674858

Efficacy of an ambulance ventilation system in reducing EMS worker exposure to airborne particles from a patient cough aerosol simulator

William G. Lindsley [a*], Francoise M. Blachere [a], Tia L. McClelland [b], Dylan T. Neu [c], Anna Mnatsakanova [d], Stephen B. Martin, Jr. [b], Kenneth R. Mead [c], and John D. Noti [a]

[a] Health Effects Laboratory Division, National Institute for Occupational Safety and Health, Centers for Disease Control and Prevention, Morgantown, West Virginia, USA

[b] Respiratory Health Division, National Institute for Occupational Safety and Health, Centers for Disease Control and Prevention, Morgantown, West Virginia, USA

[c] Division of Field Studies & Engineering, National Institute for Occupational Safety and Health, Centers for Disease Control and Prevention, Cincinnati, Ohio, USA

[d] Health Effects Laboratory Division, National Institute for Occupational Safety and Health, Centers for Disease Control and Prevention, Morgantown, West Virginia, USA

*Corresponding author:
Dr. William G. Lindsley
National Institute for Occupational Safety and Health
1000 Frederick Lane, M/S 4020
Morgantown, WV 26508
Phone: (304) 285-6336
Email: wlindsley@cdc.gov

Key words: Emergency medical services, Infection control, Ventilation systems, Airborne disease transmission, Emergency vehicle, HVAC

ABSTRACT

The protection of emergency medical service (EMS) workers from airborne disease transmission is important during routine transport of patients with infectious respiratory illnesses and would be critical during a pandemic of a disease such as influenza. However, few studies have examined the effectiveness of ambulance ventilation systems at reducing EMS worker exposure to airborne particles (aerosols). In our study, a cough aerosol simulator mimicking a coughing patient with an infectious respiratory illness was placed on a patient cot in an ambulance. The concentration and dispersion of cough aerosol particles were measured for 15 minutes at locations corresponding to likely positions of an EMS worker treating the patient. Experiments were performed with the patient cot at an angle of 0° (horizontal), 30° and 60°, and with the ambulance ventilation system set to 0, 5 and 12 air changes/hour (ACH). Our results showed that increasing the air change rate significantly reduced the airborne particle concentration ($p < 0.0001$). Increasing the air change rate from 0 to 5 ACH reduced the mean aerosol concentration by 34% (SD = 19%) overall, while increasing it from 0 to 12 ACH reduced the concentration by 68% (SD = 9%). Changing the cot angle also affected the concentration ($p < 0.0001$), but the effect was more modest, especially at 5 and 12 ACH. Contrary to our expectations, the aerosol concentrations at the different worker positions were not significantly different ($p < 0.556$). Flow visualization experiments showed that the ventilation system created a recirculation pattern which helped disperse the aerosol particles throughout the compartment, reducing the effectiveness of the system. Our findings indicate that the ambulance ventilation system reduced but did not eliminate worker exposure to infectious aerosol particles. Aerosol exposures were not significantly different at different locations within the compartment, including locations behind and beside the patient. Improved ventilation system designs with smoother and more unidirectional airflows could provide better worker protection.

INTRODUCTION

When emergency medical service (EMS) workers transport patients with contagious respiratory diseases in ambulances, the workers can be exposed to airborne particles (aerosols) containing infectious pathogens. Although EMS workers are advised to use airborne precautions when a patient has certain infectious respiratory illnesses,[1] this information about the patient may be unavailable or unclear, and the potential for the airborne transmission of many respiratory infections also is unclear or disputed.[2] In the event of a pandemic of a respiratory illness such as influenza or SARS, ambulances would be used to transport large numbers of infected patients, and EMS workers could receive a high cumulative exposure to infectious bioaerosol particles over the course of their shift. For these reasons, a better understanding of the effectiveness of measures to protect EMS workers against airborne disease transmission is needed.

Several studies have demonstrated the presence of pathogens on various surfaces in ambulances and have examined the risk of the transfer of microorganisms to EMS workers (reviewed by Hudson et al. [3]). However, research on the potential for aerosol disease transmission in ambulances has been much more limited. Luksamijarulkul and Pipitsangjan [4] found that concentrations of airborne bacteria and fungi including *Staphylococcus* and

Aspergillus species were significantly increased during patient transport in ambulances. Bielawska-Drozd et al.[5; 6] also found airborne *Staphylococcus*, *Aspergillus* and *Penicillium* species in ambulances. El Sayed et al. [7] studied reports of occupational health exposures in an urban EMS system and found that the second most common reported exposure was to tuberculosis (17%) while the third most common was to respiratory viral infections (15%).

Ventilation systems play a crucial role in reducing exposure to airborne infectious diseases.[8] However, although a large number of studies have been conducted on ventilation systems and airborne diseases in buildings,[9] studies of ambulance ventilation systems and infectious bioaerosols are far more limited; only one such report was found by us in the scientific literature. Seitz et al.[10] compared an ambulance equipped with a supplemental high efficiency particulate air (HEPA) filtration system to a standard ambulance by using aerosolized polystyrene microspheres to simulate airborne tuberculosis. They found that the modified ambulance cleared aerosol particles from the air much faster, although they noted that respiratory protection was still recommended when transporting patients with tuberculosis infections.

Guidance and standards for ambulance ventilation rates are also quite limited. Although the 2007 Federal Specification for the Star-of-Life Ambulance called for a ventilation rate of 30 air changes/hour (ACH),[11] this requirement was dropped with a 2008 change order,[12] and the ventilation rate is no longer specified. The current National Fire Protection Association (NFPA) and ASTM International standards for ambulances also do not specify ventilation rates.[13; 14] A US Department of Homeland Security guidebook recommends a minimum ventilation rate of 30 ft^3 (0.85 m^3) per minute per person if the enclosure volume is 150 ft^3 (4.25 m^3) or less per person, which would provide 24 ACH if two people were in a 150 ft^3 compartment, but no supporting information is given for this recommendation.[15]

Aerosol particles produced by coughing patients are of particular concern in disease transmission because coughing is one of the most common symptom of respiratory infections and because the violent expulsion of air during a cough generates a plume of aerosol particles that can travel 2 m or more away from an infected person.[16; 17] Several studies have shown that people expel aerosol particles containing potentially infectious microorganisms during coughing, speaking, and breathing.[18-22] Small aerosol droplets from a coughing patient can remain airborne for an extended time and can easily be inhaled.[23]

The purpose of this project is to study how an ambulance ventilation system affects EMS worker exposure to airborne particles produced by a coughing patient, and to investigate the effects of the ventilation rate, the position of an EMS worker in the ambulance, and the angle of the patient cot on worker exposure. The results presented here will help inform guidance on protecting EMS workers from airborne biohazards and suggest ways in which protective measures against exposure to bioaerosols can be improved.

METHODS

Summary

For our experiments, a cough aerosol simulator mimicking a coughing patient with a contagious respiratory infection was placed on a

patient cot in an ambulance (Figure 1). Two sets of experiments were performed. In the first, aerosol particle monitors were placed at four locations corresponding to likely positions of an EMS worker treating a patient. The simulator coughed an aerosol of KCl particles into the ambulance, and the concentration and dispersion of the aerosol particles were measured for 15 minutes. Experiments were performed with the patient cot at 0° (horizontal), 30° and 60°, and with the ambulance ventilation system set to 0, 5 and 12 air changes/hour (ACH). In the second set of experiments, an aerosol containing influenza virus was coughed into the compartment, and bioaerosol samplers were used to collect the particles for 15 minutes with the patient cot at 30° and the ventilation system set to 0, 5 and 12 ACH.

Ambulance

Our study was conducted using a 2005 Wheeled Coach Type III ambulance (Wheeled Coach, Winter Park, FL) which met the USA Federal Specification KKK-A-1822D when constructed.[24] This specification is very similar to the current construction standards for ambulances that are maintained by the US National Fire Protection Association and ASTM International.[13; 14] Type III ambulances represent about half of the US ambulance fleet. The ambulance was located outdoors during testing but was under a carport to avoid direct heating by sunlight. A schematic of the ambulance patient compartment is shown in Figure 1. An annotated photograph of the experimental set-up is shown in Figure S4 in the supplemental materials.

The ambulance patient compartment has three seats for the EMS workers: a rear-facing seat at the head of the patient cot, a seat on the left next to the control panel, and a bench seat along the right side of the compartment (shown in Figure 1 and Figure S4). The aerosol particle monitors and samplers were placed at positions corresponding to the breathing zones of EMS workers sitting on these seats. The position that a worker occupies during patient transport depends upon the tasks they are carrying out, the angle of the front of the patient cot, and the number of EMS workers in the compartment. If the front of the patient cot is raised, the worker may be on the bench seat (Positions 3-5) to treat the patient. Position 3 provides good access to the patient's head and torso if the patient cot is flat or at a shallow angle, but the EMS worker may move down the bench seat to Position 4 or 5 when the cot angle is higher. For this reason, in our experiments with the cot angle at 0° or 30°, data were collected at Positions 1-4. However, when the cot was at 60°, data were collected at Positions 1, 2, 4 and 5.

Ventilation system

The ambulance patient compartment ventilation system consists of an exhaust blower in the rear that draws air from the compartment and vents it outside, an inlet vent in the front that allows outside air to flow into the compartment, and a recirculating heater/cooler to control the air temperature. At maximum speed, the exhaust blower draws 0.7 m^3/min (25 ft^3/min) of outside air into the ambulance. Since the patient compartment has a volume of approximately 8.7 m^3 (308 ft^3), this corresponds to about 5 ACH (the air change rate is the flow rate of air into and out of the compartment divided by the volume of the compartment). The heater/cooler recirculates up to 12 m^3/minute of air but does not filter the air, nor does it exchange inside air for outside air. The heater/cooler was not used in this study.

For our experiments, the exhaust blower was replaced with a recirculating HEPA filtration system (FS4010, Flow Sciences, Leland, NC) connected to the compartment inlet and outlet in order to avoid bringing aerosol particles in from outside of the ambulance and to allow the background aerosol concentration in the ambulance to be reduced to near zero before each experiment. The HEPA filtration system was set to 0 ACH, 5 ACH (matching the original exhaust blower), or 12 ACH (1.8 m^3/minute). The current US ambulance standards [13; 14] do not specify an air change rate for ambulance patient compartments, but 12 ACH is the recommended ventilation rate for an airborne infection isolation room in a healthcare facility.[25] The air change rates through the HEPA filtration system were measured using an anemometer (VelociCalc Rotating Vane Anemometer 5725, TSI, Shoreview, MN). The 0, 5 and 12 ACH ventilation system air change rates do not include air infiltrating from the outside into the compartment due to natural convention through gaps and seams. Air infiltration was minimized by sealing all exterior doors, windows and openings leading into the patient compartment with tape or foam. The air infiltration rate into the sealed compartment was measured twice using the tracer gas constant decay method with sulfur hexafluoride as the tracer and the concentration measured using two photoacoustic gas analyzers (Innova Model 1412, Lumasense Technologies, Santa Clara, CA).[26]

Virus and cell stock

Influenza strain A/WS/33 (H1N1, ATCC VR-825) and Madin-Darby canine kidney (MDCK) cells (ATCC CCL-34) were purchased from the American Type Culture Collection (ATCC, Manassas, VA) and maintained as described previously.[27] The influenza virus was propagated in Complete Dulbecco's Modified Eagle Medium (CDMEM) consisting of Dulbecco's Modified Eagle medium, 100 U/mL penicillin G, 100 µg/mL streptomycin, 2 mM L-glutamine, 0.2% bovine serum albumin, and 25mM HEPES buffer (Life Technologies, Grand Island, NY).

Cough aerosols

Our study was conducted using a modified version of the NIOSH cough aerosol simulator described previously.[23; 28] The flow rate of the simulated cough was based on cough flow profiles recorded from influenza patients and had a volume of 4.2 liters with a peak flow rate of 11 L/s.[28] The mouth of the cough simulator was 65 cm (25.5 inches) above the base of the cough simulator (shown in the supplemental material, Figure S1). The cough aerosol output from the cough simulator was measured using a spray droplet size analyzer (Spraytec Analyzer with an Inhalation Cell, Malvern Instruments Ltd., Malvern, UK) as described previously.[28] A schematic of the cough aerosol simulator and information about the cough aerosol output are shown in the supplemental materials.

For experiments in which the aerosol concentration was monitored using optical aerosol particle counters (OPCs), the cough aerosol was generated by nebulizing a 28% KCl solution using a single-jet Collison nebulizer (BGI, Butler, NJ) at 14 kPa (20 lbs./in^2), passing the aerosol through a diffusion drier (Model 3062, TSI, Shoreview, MN), and mixing it with 8.1 L/min of dry filtered air. Aerosol particle concentrations were measured using optical aerosol particle counters (OPCs; Model 1.108, GRIMM Technologies, Douglasville, GA). The OPCs were controlled by a laptop computer

running a custom-written LabVIEW program (National Instruments, Austin, Texas) through a wireless RS-232 interface (Parani SD1000 and UD100, Sena Technologies, Seoul, Korea). The GRIMMs were programed to report particle counts/liter in eight size bins from 0.3 to 3 µm at a rate of once per second.

For experiments using influenza virus, the virus was diluted in modified Hank's Balanced Salt Solution (MHBSS), which consists of HBSS supplemented with 0.1% bovine serum albumin (BSA) (Sigma–Aldrich, St. Louis, MO), 100 units/mL penicillin G and 100 units/mL streptomycin (Invitrogen, Carlsbad, CA). The nebulizer solution had a viral concentration of 4.46×10^7 viral copies/mL. The cough aerosol was generated by nebulizing the virus solution using a micropump nebulizer (Aeroneb AG-AL7000SM, Aerogen, Chicago, IL). The virus aerosol was mixed with 2 L/min of dry filtered air, passed through the diffusion drier, and mixed with an additional 7 L/min of dry filtered air. The viral aerosols were collected in the patient compartment using bioaerosol samplers (BioSampler, SKC, Eighty-four, PA). The flowrate through the SKC BioSamplers is controlled by three critical orifices. The mean flowrate through our set of BioSamplers is 13.2 L/min (standard deviation 0.62). The vacuum for each sampler was supplied by a Gast DOA-P704 vacuum pump (Gast Manufacturing, Benton Harbor, MI).

Test procedure

Two types of experiments were performed: Measurements of the aerosol particle volume concentration over time, and collection of airborne influenza virus.

For the aerosol volume concentration measurements, the cot angle was set to 0°, 30° or 60°. For experiments with the patient cot at 0° or 30°, optical aerosol particle counters were placed in positions 1-4 as shown in Figure 1. For experiments with the cot at 60°, the OPCs were placed in positions 1, 2, 4 and 5 in order to include a location further down the bench seat where an EMS worker might be when the patient is more upright. The cough simulator nebulizer was loaded with 28% KCl. The HEPA system was run at its maximum rate to reduce the aerosol concentration as much as possible, and a fan was used to increase air mixing. After 45 minutes, the fan was turned off and the HEPA system was set to the rate to be used in the experiment (0, 5 or 12 ACH). The air movement in the compartment was allowed to stabilize for 10 minutes, during which time the OPCs measured background concentration levels. The cough aerosol simulator then coughed once into the compartment. After each cough from the simulator, the number concentrations of aerosol particles with optical diameters from 0.3 to 3 µm were measured for 15 minutes at 1 Hz using the OPCs. The number concentrations were converted to volume concentrations as described below. Four replicate experiments were conducted for each combination of cot angle and ventilation rate (36 experiments total). Within the experimental replicates, the four OPCs were rotated among the four positions so that each OPC was in each position once.

For experiments with airborne influenza virus, the procedure was similar, but the OPCs in positions 1 and 4 were replaced with BioSamplers containing 20 mL of MHBSS. The HEPA system and fan were run for 30 minutes and then the air movement was allowed to stabilize for 10 minutes before coughing. The BioSamplers were started a few minutes before the simulator coughed, and aerosol collection continued for 15 minutes after each cough. After the aerosol collection was completed, the

bioaerosol collection was stopped and the HEPA system and fan were run for 30 minutes to clear the airborne virus in the compartment before the bioaerosol samples were retrieved. Experiments were conducted with the HEPA system at 0, 5 and 12 ACH and with the cot at 30° only. Three replicates were conducted for each air change rate for a total of nine experiments.

Influenza virus RNA isolation and qPCR detection

Viral RNA was isolated from the collected aerosol samples using the MagMAX™ Viral RNA Isolation kit (Thermo Fisher Scientific, Waltham, MA, USA) as described by Blachere et al.[29] In brief, one mL (5%) of the collected aerosol sample was supplemented with a 1:1 volume of 2-propanol (Sigma). The manufacturer's instructions were followed for the remainder of the viral RNA isolation procedure. Viral RNA was eluted with 30 µL of elution buffer and transcribed into cDNA using the High Capacity cDNA Reverse Transcription Kit (Thermo Fisher Scientific).

Molecular analysis of viral-laden cough aerosols was performed using quantitative polymerase chain reaction (qPCR) targeting the matrix 1 (M1) gene of influenza strain A/WS/33, as previously described.[29] A 5 µL (12.5%) cDNA volume was analyzed per sample, in duplicate.

Data analysis

When fluids such as lung secretions are aerosolized, the number of pathogens that an aerosol particle can carry depends upon the volume of the particle; larger particles can carry more pathogens. As a result, the aerosol volume concentration (total volume of aerosol particles per unit volume of air) gives a better indication of the amount of airborne infectious material to which a worker is potentially exposed than does the number concentration (total number of aerosol particles per unit volume of air). [30-32] For this reason, the aerosol concentration data reported in this paper are in volume concentration. The volume concentration is analogous to the more commonly used mass concentration; if the aerosol particles have a constant density, the mass concentration is simply the volume concentration multiplied by the density of the particles. A more detailed explanation of the volume concentration is provided in the supplemental materials.

The optical particle counters report the number of aerosol particles detected per liter of air (#/L) in eight logarithmically-spaced size bins from 0.3 to 3 µm. The background aerosol number concentration was calculated based on the mean number concentration in each size bin during the three minutes before the cough and was subtracted from the concentrations measured after the cough. The volume of the aerosol in each size bin per m^3 of air (volume concentration) was calculated by multiplying the particle count by the volume of an individual particle with the mean diameter of the size bin, assuming the particles were spherical. The total aerosol volume/m^3 (total aerosol volume concentration) was found by summing the aerosol volume concentrations for all the size bins. The mean volume concentration was found by averaging the total volume concentration over 15 minutes starting from the time of the cough.

The total volume of aerosol expelled by the cough aerosol simulator changes with the cot angle (shown in the supplemental material, Table S1), although the size distribution does not change noticeably. The output at 0° is about 7% higher compared to 30°, while the output at 60°

is 14% lower. To control for this variation in output, the volume concentrations at 0° and 60° were normalized to the 30° concentrations by dividing them by a normalization factor:

$$Normalization\ factor = \frac{cough\ aerosol\ output\ at\ experiment\ cot\ angle}{cough\ aerosol\ output\ at\ 30°\ cot\ angle} \quad (1)$$

In the Results, "concentration" always refers to the normalized volume concentrations.

Due to the skewed nature of the concentration data, a natural logarithm transformation was performed prior to the analysis. Because measurements were made at Positions 1, 2, 3 and 4 when the cot angle was 0° or 30° and at Positions 1, 2, 4 and 5 when the cot angle was 60°, an initial analysis of the overall effect of position on mean volume concentration was performed, which showed that the position did not have a significant effect. Following this, a two-factor factorial design was used to examine the effects of the angle of the patient cot (three levels: 0°, 30° or 60°), air exchange rate (three levels: 0, 5 or 12) and their interaction at each position. If significant differences were found, Tukey's multiple comparison test was used to determine which means were significantly different from the rest. All possible multiple comparison tests were performed for each combination of cot angle (0°, 30° and 60°) and air change rate (0, 5 and 12 ACH). The data were analyzed using SAS 9.4 (SAS Institute, Inc., Cary, NC). The SAS analysis of the results is shown in the Supplemental Materials.

Supplemental on-line material

A supplemental file for this article is available on-line. It includes a schematic of the cough simulator, an annotated photograph of the experimental set-up, additional graphs and explanatory material, a table providing the experimental data, and the SAS output.

RESULTS

Cough aerosol volume concentration over time

The aerosol volume concentrations over time at position 1 are shown for the 30° cot angles in Figure 2. At 0 air changes/hour, the aerosol concentration tended to level off after a few minutes, while the concentration declined over time at 5 ACH and declined more rapidly at 12 ACH. Results for all positions and cot angles are shown in the supplemental material. Some differences can be seen at different cot angles for 0 ACH, but the concentration curves are fairly similar at the different cot angles for 5 ACH and 12 ACH.

Mean aerosol volume concentration

The mean aerosol volume concentrations over the 15-minute test interval are shown in Figure 3 for each position, cot angle and air change rate. Changes in the air change rate had a significant effect on the aerosol concentration ($p < 0.0001$). For example, at position 1 with the cot at 0°, the mean aerosol concentration at 5 ACH was 64% (standard deviation, SD = 10%) of the 0 ACH concentration, and at 12 ACH the mean concentration was 32% (SD = 5.4%) of the 0 ACH value. The air change rate had similar effects at the other positions and cot angles. Overall, for all positions and angles combined, the 5 ACH flowrate reduced the mean concentration to 66% (SD = 19%) of the 0 ACH value, while 12 ACH reduced the mean concentration to 34% (SD = 9.3%) of the 0 ACH level. The aerosol volume concentrations also were affected by changes in the cot angle ($p <$

0.0001), although the effects were more modest, especially at 5 and 12 ACH. For example, at position 4 with 0 ACH, the concentration with the cot at 30° increased to 128% (SD = 28%) of the concentration at a 0° angle, while the concentration with the cot at 60° decreased to 75% (SD = 11%) of the 0° level. On the other hand, the position of the particle counter in the patient compartment did not have a significant effect on the concentration ($p = 0.556$). For example, at a 30° cot angle with 12 ACH, the mean concentrations at positions 2, 3 and 4 were 95% (SD = 11%), 95% (SD = 13%) and 93% (SD = 7.3%) of the position 1 concentration. The statistical interaction between ACH and cot angle was significant ($p = 0.0031$ for position 1, $p < 0.0001$ for positions 2 and 4). Graphs showing the data with different groupings of bars are shown in the supplemental materials

Exposure to airborne influenza virus

The cough aerosol simulator was used to cough an aerosol containing influenza virus into the patient compartment, and the viral aerosol was collected for 15 minutes at positions 1 and 4. The amount of airborne virus detected (viral M1 copies/m^3 of air) is shown in Figure 4. Similar to the results seen in Figure 3, the air change rate had a significant effect on the amount of airborne virus ($p = 0.0001$), while the two positions were not significantly different ($p = 0.850$). In position 1, the amounts of airborne virus at 5 ACH and 12 ACH were 71% (SD = 21%) and 43% (SD = 7.0%) of the 0 ACH value, while in position 4 they were 60% (SD = 30%) and 29% (SD = 10%)

Environmental conditions

For the experiments using KCl aerosols, the overall mean temperature inside the patient compartment was 26°C (SD = 2.1) and the mean relative humidity was 60% (SD = 5.4). For the influenza virus experiments, the mean interior temperature was 26°C (SD = 1.9) and the mean humidity was 67% (SD = 2.5). The air infiltration rate into the sealed compartment was 0.26 ACH (SD 0.04; n = 2) with the ventilation system off.

DISCUSSION

EMS workers transport patients with a variety of infectious diseases, including some that can be spread by airborne particles. Patients are typically in an EMS transport vehicle for a relatively short time; in the US, average ambulance transport times are 11 minutes in urban and suburban regions and 17 minutes in rural areas.[33] However, even a short exposure to a high concentration of an infectious bioaerosol can result in infection, and longer transport times are not uncommon. In addition, during a respiratory disease pandemic, workers would be transporting multiple infected patients to health care facilities over the course of their shift, and their cumulative exposures could be substantial. The use of ventilation to reduce exposure to airborne contaminants in buildings has been widely studied, but in ambulances such studies have been far more limited. Although the same principles apply to both settings, ambulances are cramped spaces with much less air volume per person than a typical patient room in a medical facility, which greatly increases the potential exposure to infectious aerosols. In addition, ambulances have ventilation systems that are quite different from hospital rooms. Thus, ventilation studies need to be done specifically in ambulances in order to understand the risks to EMS workers and the effects of different parameters such as worker location, patient position, ventilation rate and the effectiveness of ventilation designs to use

dilution and directed airflows to protect against worker exposures.

As can be seen in Figure 2, when a patient coughs into the ambulance compartment, the cough results in a rapid initial increase in the aerosol particle volume concentration. With no mechanical ventilation, the aerosol concentration levels off after a few minutes, while the concentration gradually declines at 5 ACH and declines more rapidly at 12 ACH. Thus, the ventilation system does reduce exposure to bioaerosols, but only gradually over time, and some worker exposure is unavoidable. This can also be seen in Figure 3, which shows the aerosol volume concentration averaged over 15 minutes. The ventilation system clearly reduces the exposure to bioaerosols, and the reduction is more rapid at a higher ventilation rate, but significant worker exposure still occurs in every position. It should also be noted that the experiments presented here tracked the aerosol concentration after a single cough; if a patient were coughing every few minutes or was exhaling airborne pathogens, as is common, the bioaerosol content of the compartment would be constantly renewed and the mean concentrations would be higher.

Contrary to our expectations, Figure 3 also shows that while the mean aerosol volume concentrations were somewhat different at the different worker locations in the ambulance at 0 ACH, the mean concentrations at 5 ACH and 12 ACH were very similar from position to position. Similarly, at 0 ACH, the aerosol concentrations were lower at each position with the cot at 60° compared to 0° or 30°, presumably because when the simulator was more upright, the cough was directed more toward the rear of the ambulance. However, when the air change rate was 5 ACH or 12 ACH, changing the cot angle had only a small effect on the mean aerosol concentrations. These outcomes can also be seen in Figure 4; tests using an influenza virus aerosol showed that increasing the air change rate to 5 and 12 ACH significantly reduced the amount of virus collected at positions 1 and 4, but at each air change rate there was no significant difference between the two positions.

These results seemed counter-intuitive; we anticipated that the worker positions at the head of the patient cot would receive lower aerosol concentrations, especially as the cot angle increased and the cough was directed more toward the rear of the ambulance. However, an investigation using smoke visualization of the airflow patterns in the patient compartment revealed that, because the airflows into the ambulance from a small inlet on the right-hand side at the front (Figure 1), the air forms a jet along the right side that generates a clockwise recirculation pattern (Figure 5) spanning the compartment. This recirculation carried air from the rear of the ambulance along the left side and toward the front of the compartment, sweeping aerosol particles from the back toward the front of the ambulance. Thus, the air mixing caused by the cough itself and the circulation pattern created by the ventilation system caused a high degree of air mixing and quickly distributed the cough aerosol throughout the compartment. This effect can be seen in Figure 2. In position 1, with the cot at 30°, the aerosol concentration peaks earlier after the cough as the airflow rate increases to 5 ACH, and even earlier at 12 ACH. The earlier peaks indicate that the aerosol is being carried more rapidly from the rear of the ambulance toward the front as the airflow increases.

This observation provides an important lesson for designing ambulance ventilation

systems to reduce aerosol exposure: It is not sufficient to simply blow air into a patient compartment at the chosen air change rate. The airflow patterns need to be analyzed and the ventilation system designed so that the air is swept away from the patient and worker and toward an outlet. For example, a laminar airflow system with air entering from a broad inlet in the ceiling and exiting at the floor could be used to quickly sweep particles downward below the breathing zone of the worker while avoiding air mixing or recirculation. Alternatively, it may be possible to design a laminar flow system with air flowing from the front to the back of the ambulance, although this could be problematic if the worker needs to be downstream of the patient. Vertical and horizontal laminar airflow systems are now used in operating rooms to prevent contamination of surgical sites by airborne particles settling into wounds.[34] Similar concepts could potentially be applied to ambulances to reduce the inhalation exposure of workers to airborne pathogens, although ambulances have significant space constraints compared to buildings. It should be emphasized that any new ventilation system will need to be carefully tested and evaluated to ensure that it is actually providing the needed protection from bioaerosols.

Finally, the limitations of our study need to be acknowledged. First, the optical particle counters measured airborne particles from 0.3 to 3 μm, which covers many of the bioaerosol particles that are small enough to remain airborne for an extended time but large enough to carry pathogens. However, humans do produce aerosol particles across a very broad size range that carry pathogens,[35] and particles outside our test size range would behave differently. Second, the cough aerosol simulator and the particle counters are at ambient temperature, not body temperature, and thus do not create the thermal convection currents that people would generate. Third, the conversion from particle counts to particle volume used to analyze our data is commonly used but should be regarded as an approximation. Fourth, the particle counters and aerosol samplers were kept in fixed locations during our experiments, while EMS workers may move during patient transport, which could affect particle movement and the worker's exposure. Finally, our ambulance was stationary during our tests and all openings to the exterior were sealed; thus, any additional ventilation effects that would occur due to air infiltration into a moving ambulance were not included in our study.

CONCLUSIONS

The protection of EMS workers from airborne disease transmission is important during routine transport of patients with infectious respiratory illnesses and would be critical during a respiratory disease pandemic. Thus, a better understanding of exposure control devices such as ambulance ventilation systems is needed. Our results show that an ambulance ventilation system does reduce EMS worker exposure to infectious aerosol particles produced by patients, but the systems may still allow significant exposure to occur even at relatively high air change rates. Our results also indicate that aerosol exposure can occur at all locations within the compartment, and that locations behind or beside the patient cannot be assumed to be safe from airborne particles. Finally, our results suggest that improved ventilation system designs with smoother and more unidirectional airflows could provide better worker protection.

ACKNOWLEDGEMENTS

This research was funded by the Office of Public Health Preparedness and Response (OPHPR) of the US Centers for Disease Control and Prevention (CDC). The National Institute for Occupational Safety and Health (NIOSH) is a part of the CDC. The findings and conclusions in this report are those of the authors and do not necessarily represent the official position of NIOSH, CDC. Mention of any company or product does not constitute endorsement by NIOSH, CDC.

REFERENCES

1. Isakov A, Hick J and team T. *EMS Infectious Disease Playbook.* US Department of Health and Human Services 2017, 86 p. Available at https://www.ems.gov/pdf/ASPR-EMS-Infectious-Disease-Playbook-June-2017.pdf.

2. Kutter JS, Spronken MI, Fraaij PL, Fouchier RA and Herfst S. Transmission routes of respiratory viruses among humans. *Curr Opin Virol* 28: 142-51, 2018. https://www.ncbi.nlm.nih.gov/pubmed/29452994

3. Hudson AJ, Glaister GD and Wieden HJ. The Emergency Medical Service Microbiome. *Appl Environ Microbiol* 84: e02098-17, 2018. https://www.ncbi.nlm.nih.gov/pubmed/29222105

4. Luksamijarulkul P and Pipitsangjan S. Microbial air quality and bacterial surface contamination in ambulances during patient services. *Oman Med J* 30: 104-10, 2015. https://www.ncbi.nlm.nih.gov/pubmed/25960835

5. Bielawska-Drozd A, Cieslik P, Wlizlo-Skowronek B, Winnicka I, Kubiak L, Jaroszuk-Scisel J, Depczynska D, Bohacz J, Kornillowicz-Kowalska T, Skopinska-Rozewska E and Kocik J. Identification and characteristics of biological agents in work environment of medical emergency services in selected ambulances. *Int J Occup Med Environ Health* 30: 617-27, 2017. https://www.ncbi.nlm.nih.gov/pubmed/28584319

6. Bielawska-Drozd A, Cieslik P, Bohacz J, Kornillowicz-Kowalska T, Zakowska D, Bartoszcze M, Wlizlo-Skowronek B, Winnicka I, Brytan M, Kubiak L, Skopinska-Rozewska E and Kocik J. Microbiological analysis of bioaerosols collected from Hospital Emergency Departments and ambulances. *Ann Agric Environ Med* 25: 274-9, 2018. https://www.ncbi.nlm.nih.gov/pubmed/29936812

7. El Sayed M, Kue R, McNeil C and Dyer KS. A descriptive analysis of occupational health exposures in an urban emergency medical services system: 2007-2009. *Prehosp Emerg Care* 15: 506-10, 2011. https://www.ncbi.nlm.nih.gov/pubmed/21797786

8. Hodgson MJ, Miller SL, Li Y, McCoy WF, Parsons SA, Schoen LJ and Sekhar C. *ASHRAE Position Document on Airborne Infectious Diseases.* ASHRAE 2009, 17 p. Available at https://www.ashrae.org/File%20Library/About/Position%20Documents/Airborne-Infectious-Diseases.pdf.

9. Luongo JC, Fennelly KP, Keen JA, Zhai ZJ, Jones BW and Miller SL. Role of mechanical ventilation in the airborne transmission of infectious agents in buildings. *Indoor Air* 26: 666-78, 2016. https://www.ncbi.nlm.nih.gov/pubmed/26562748

10. Seitz TA, Decker JA and Jensen PA. *University of Medicine and Dentistry of New Jersey, University Hospital Newark, New Jersey.* NIOSH HETA 95–0031–2601. 1996, 12 p. Available at https://www.cdc.gov/niosh/hhe/reports/pdfs/1995-0031-2601.pdf.

11. GSA. *KKK-A-1822F Federal Specification for the Star-of-Life Ambulance.* Washington, DC: US General Services Administration, 2007. WWW.GSA.GOV/AUTOMOTIVE

12. GSA. *KKK-A-1822F Federal Specification for the Star-of-Life Ambulance Change Notice 1.* Washington, DC: US General Services Administration, 2008. WWW.GSA.GOV/AUTOMOTIVE

13. NFPA. *NFPA 1917 Standard for Automotive Ambulances.* Quincy, MA: National Fire Protection Association, 2013.

14. ASTM. *ASTM F2020-2A Standard Practice for Design, Construction, and Procurement of Emergency Medical Services Systems (EMSS) Ambulances.* West Conshohocken, PA: ASTM International, 2009.

15. Avery L, Jacobs A, Moore J, Boone C and Malone T. *Ambulance Patient Compartment Human Factors Design Guidebook.* US Department of Homeland Security GS-10-F-0181J. 2015, 102 p. Available at https://www.dhs.gov/publication/ambulance-patient-guidebook.

16. Zhu S, Kato S and Yang J-H. Study on transport characteristics of saliva droplets produced by coughing in a calm indoor environment. *Build Environ* 41: 1691-702, 2006. https://doi.org/10.1016/j.buildenv.2005.06.024

17. Tang JW, Nicolle AD, Pantelic J, Jiang M, Sekhr C, Cheong DK and Tham KW. Qualitative real-time schlieren and shadowgraph imaging of human exhaled airflows: an aid to aerosol infection control. *PLoS ONE* 6: e21392, 2011. https://www.ncbi.nlm.nih.gov/pubmed/21731730

18. Fabian P, McDevitt JJ, DeHaan WH, Fung RO, Cowling BJ, Chan KH, Leung GM and Milton DK. Influenza virus in human exhaled breath: an observational study. *PLoS ONE* 3: e2691, 2008. https://www.ncbi.nlm.nih.gov/pubmed/18628983

19. Lindsley WG, Blachere FM, Beezhold DH, Thewlis RE, Noorbakhsh B, Othumpangat S, Goldsmith WT, McMillen CM, Andrew ME, Burrell CN and Noti JD. Viable influenza A virus in airborne particles expelled during coughs versus exhalations. *Influenza Other Respir Viruses* 10: 404-13, 2016. https://www.ncbi.nlm.nih.gov/pubmed/26991074

20. Yan J, Grantham M, Pantelic J, Bueno de Mesquita PJ, Albert B, Liu F, Ehrman S, Milton DK and Consortium E. Infectious virus in exhaled breath of symptomatic

seasonal influenza cases from a college community. *Proc Natl Acad Sci USA* 115: 1081-6, 2018. https://www.ncbi.nlm.nih.gov/pubmed/29348203

21. Fennelly KP, Jones-Lopez EC, Ayakaka I, Kim S, Menyha H, Kirenga B, Muchwa C, Joloba M, Dryden-Peterson S, Reilly N, Okwera A, Elliott AM, Smith PG, Mugerwa RD, Eisenach KD and Ellner JJ. Variability of infectious aerosols produced during coughing by patients with pulmonary tuberculosis. *Am J Respir Crit Care Med* 186: 450-7, 2012. https://www.ncbi.nlm.nih.gov/pubmed/22798319

22. Patterson B, Morrow C, Singh V, Moosa A, Gqada M, Woodward J, Mizrahi V, Bryden W, Call C, Patel S, Warner D and Wood R. Detection of Mycobacterium tuberculosis bacilli in bio-aerosols from untreated TB patients. *Gates Open Res* 1: 11, 2017. https://www.ncbi.nlm.nih.gov/pubmed/29355225

23. Lindsley WG, King WP, Thewlis RE, Reynolds JS, Panday K, Cao G and Szalajda JV. Dispersion and exposure to a cough-generated aerosol in a simulated medical examination room. *J Occup Environ Hyg* 9: 681-90, 2012. https://www.ncbi.nlm.nih.gov/pubmed/23033849

24. GSA. *KKK-A-1822E Federal Specification for the Star-of-Life Ambulance.* US General Services Administration, 2002. www.gsa.gov/automotive

25. ASHRAE. *ANSI/ASHRAE/ASHE Standard 170-2017 Ventilation of health care facilities.* Atlanta, GA: ASHRAE, 2017.

26. ASTM. *ASTM E741-11 (Reapproved 2017) Standard Test Method for Determining Air Change in a Single Zone by Means of a Tracer Gas Dilution.* West Conshohocken, PA: ASTM International, 2017.

27. Blachere FM, Cao G, Lindsley WG, Noti JD and Beezhold DH. Enhanced detection of infectious airborne influenza virus. *J Virol Methods* 176: 120-4, 2011. https://www.ncbi.nlm.nih.gov/pubmed/21663766

28. Lindsley WG, Reynolds JS, Szalajda JV, Noti JD and Beezhold DH. A Cough Aerosol Simulator for the Study of Disease Transmission by Human Cough-Generated Aerosols. *Aerosol Sci Technol* 47: 937-44, 2013. https://www.ncbi.nlm.nih.gov/pubmed/26500387

29. Blachere FM, Lindsley WG, Weber AM, Beezhold DH, Thewlis RE, Mead KR and Noti JD. Detection of an avian lineage influenza A(H7N2) virus in air and surface samples at a New York City feline quarantine facility. *Influenza Other Respir Viruses* 12: 613-22, 2018. https://www.ncbi.nlm.nih.gov/pubmed/29768714

30. Pan M, Carol L, Lednicky JA, Eiguren-Fernandez A, Hering S, Fan ZH and Wu CY. Determination of the distribution of infectious viruses in aerosol particles using water-based condensational growth technology and a bacteriophage MS2 model. *Aerosol Sci Technol* 53: 583-93, 2019. https://www.ncbi.nlm.nih.gov/pubmed/31359905

31. Walls HJ, Ensor DS, Harvey LA, Kim JH, Chartier RT, Hering SV, Spielman SR and Lewis GS. Generation and sampling of nanoscale infectious viral aerosols. *Aerosol Sci Technol* 50: 802-11, 2016. http://dx.doi.org/10.1080/02786826.2016.1191617

32. Zuo Z, Kuehn TH, Verma H, Kumar S, Goyal SM, Appert J, Raynor PC, Ge S and Pui DYH. Association of Airborne Virus Infectivity and Survivability with its Carrier Particle Size. *Aerosol Sci Technol* 47: 373-82, 2013. <Go to ISI>://WOS:000321170400003

33. Carr BG, Caplan JM, Pryor JP and Branas CC. A meta-analysis of prehospital care times for trauma. *Prehosp Emerg Care* 10: 198-206, 2006. https://www.ncbi.nlm.nih.gov/pubmed/16531377

34. Jain S and Reed M. Laminar Air Flow Handling Systems in the Operating Room. *Surg Infect (Larchmt)* 20: 151-8, 2019. https://www.ncbi.nlm.nih.gov/pubmed/30596534

35. Gralton J, Tovey E, McLaws ML and Rawlinson WD. The role of particle size in aerosolised pathogen transmission: a review. *J Infect* 62: 1-13, 2011. https://www.ncbi.nlm.nih.gov/pubmed/21094184

FIGURES

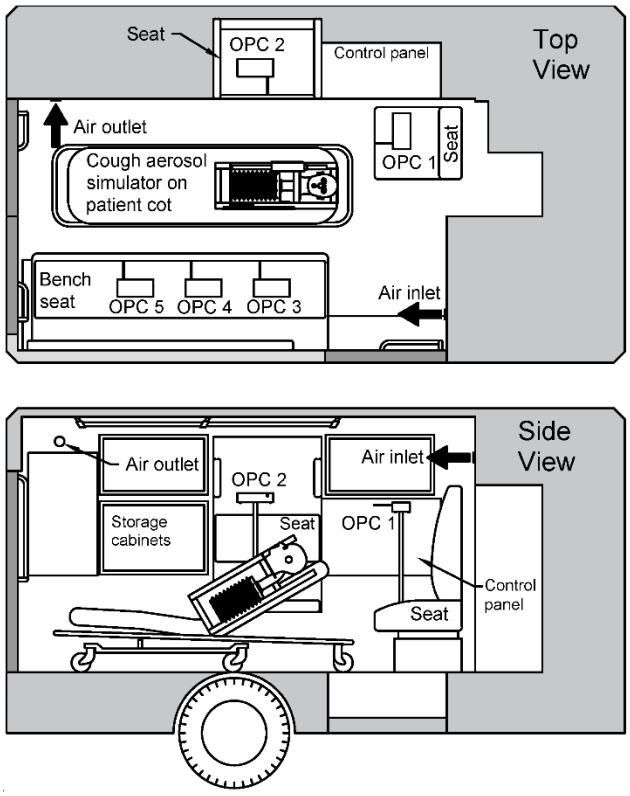

Figure 1: Ambulance patient compartment. The patient cot was adjusted so that the cough simulator was at 0° (horizontal), 30° (as shown in the figure) or 60°. For each test, four optical particle counters (OPCs) were placed in locations representing possible positions for a seated EMS worker treating the patient. OPCs were placed in the positions labeled OPC 1-4 when the cot was at 0° or 30°, and positions OPC 1, 2, 4 and 5 when the cot was at 60°. The inlet of each OPC was placed 70 cm (27 9/16”) above the seat cushion and even with the front of the cushion to place it within the breathing zone of a seated EMS worker. An annotated photograph of the set-up is shown in Figure S4 in the supplemental materials.

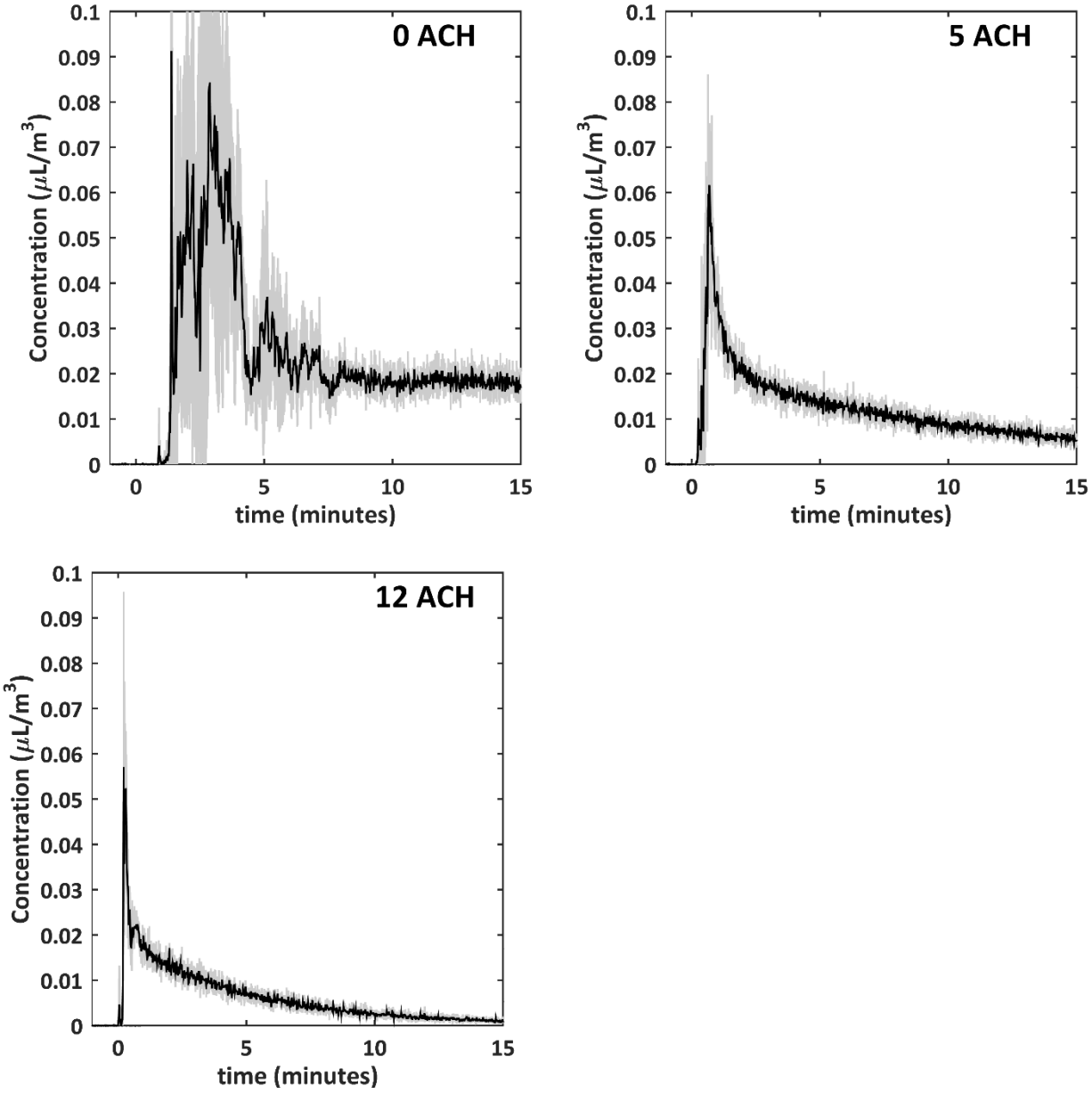

Figure 2: Aerosol volume concentration over time at position 1 with the cot at 30° at air change rates of 0, 5 and 12 ACH. The aerosol volume concentration is the total volume of KCl aerosol particles from 0.3 to 3 µm in diameter per m^3 of air. Each line is the mean of four experiments. The gray shading shows the standard deviation.

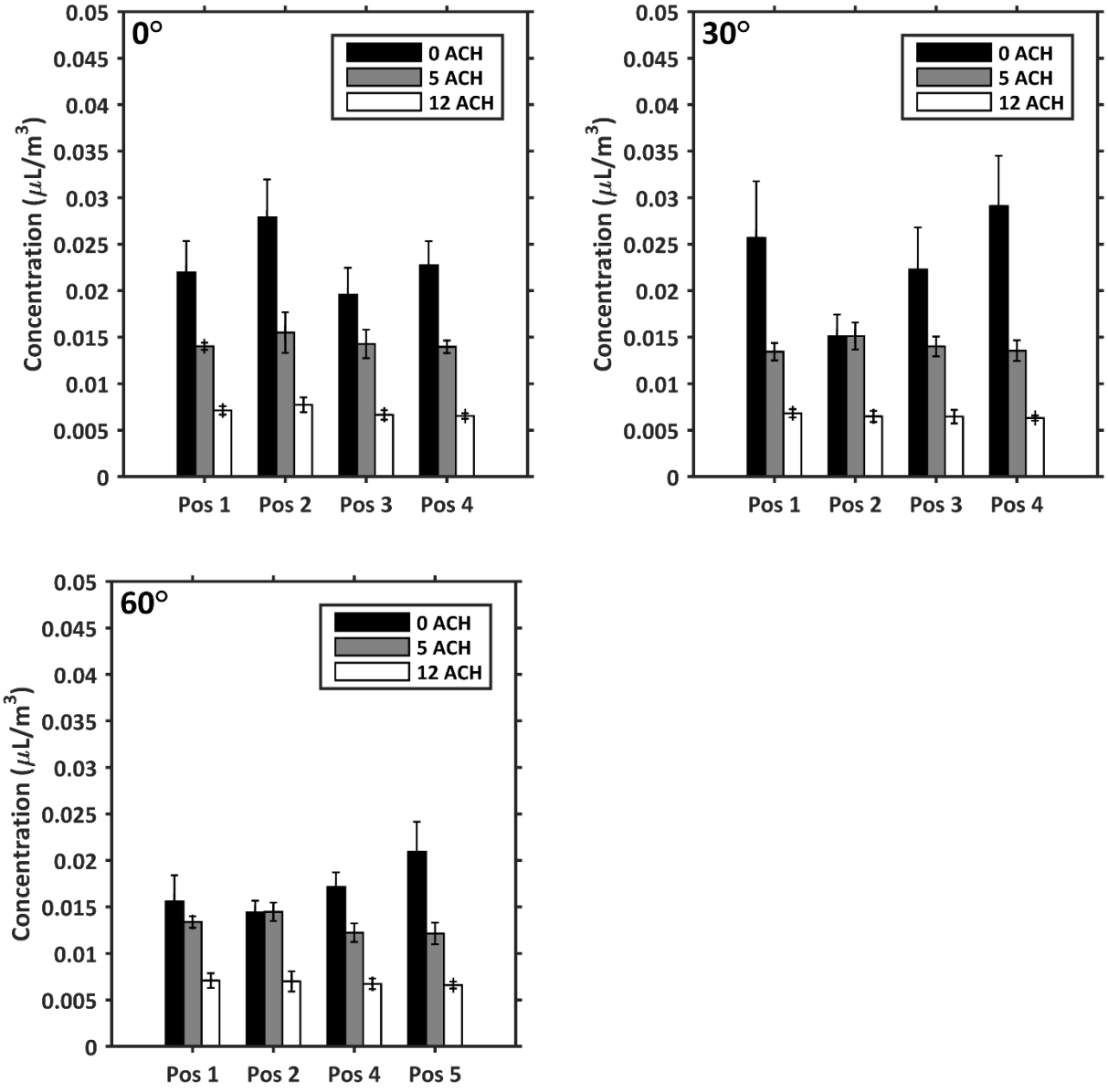

Figure 3: Mean aerosol particle volume concentration over 15 minutes at each position and air change rate with the cot at 0°, 30° and 60°. Each bar shows the mean and standard deviation of four experiments using 28% KCl. The air change rate and cot angle had a significant effect on the mean concentrations ($p < 0.0001$ for both), while results at different positions were not significantly different ($p = 0.556$).

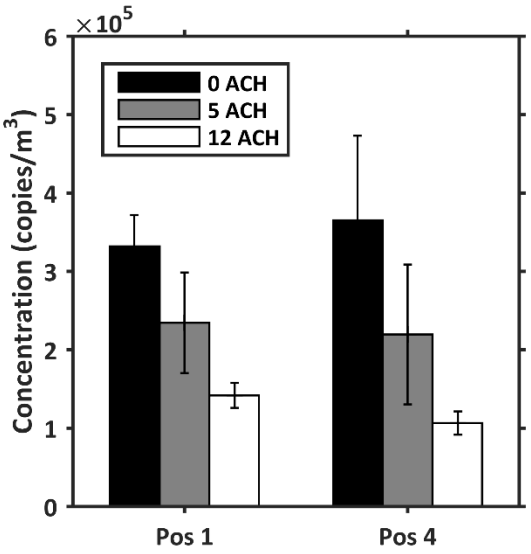

Figure 4: Airborne influenza virus concentration in viral M1 copies/m^3 of air. Airborne virus was collected for 15 minutes after each cough. The patient cot was at a 30° angle. Each bar shows the mean and standard deviation of three experiments. The air change rate had a significant effect on the mean concentration ($p < 0.0001$), while the OPC position did not ($p = 0.850$).

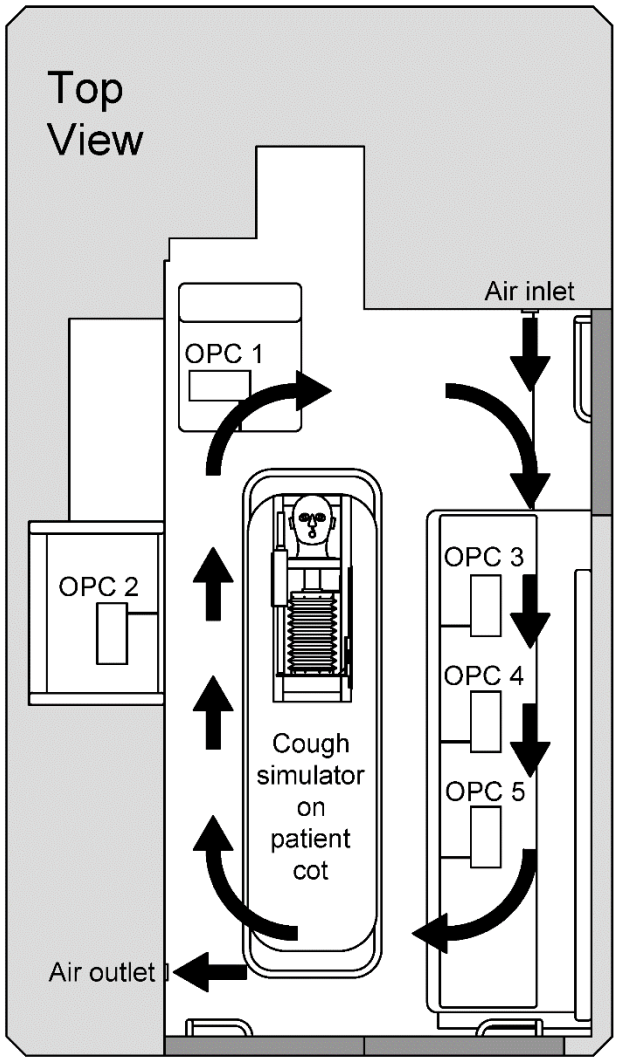

Figure 5: Air circulation pattern in the ambulance patient compartment generated by the ventilation system. The jet of air created by the air inlet causes a clockwise recirculation pattern to form which circulates aerosol particles throughout the compartment. Even if the cough is directed toward the rear of the ambulance, aerosol particles are carried toward the front by the recirculation. Thus, a worker anywhere in the ambulance is exposed to the cough aerosol particles.

Efficacy of an ambulance ventilation system in reducing EMS worker exposure to airborne particles from a patient cough simulator

Online Supplemental Materials

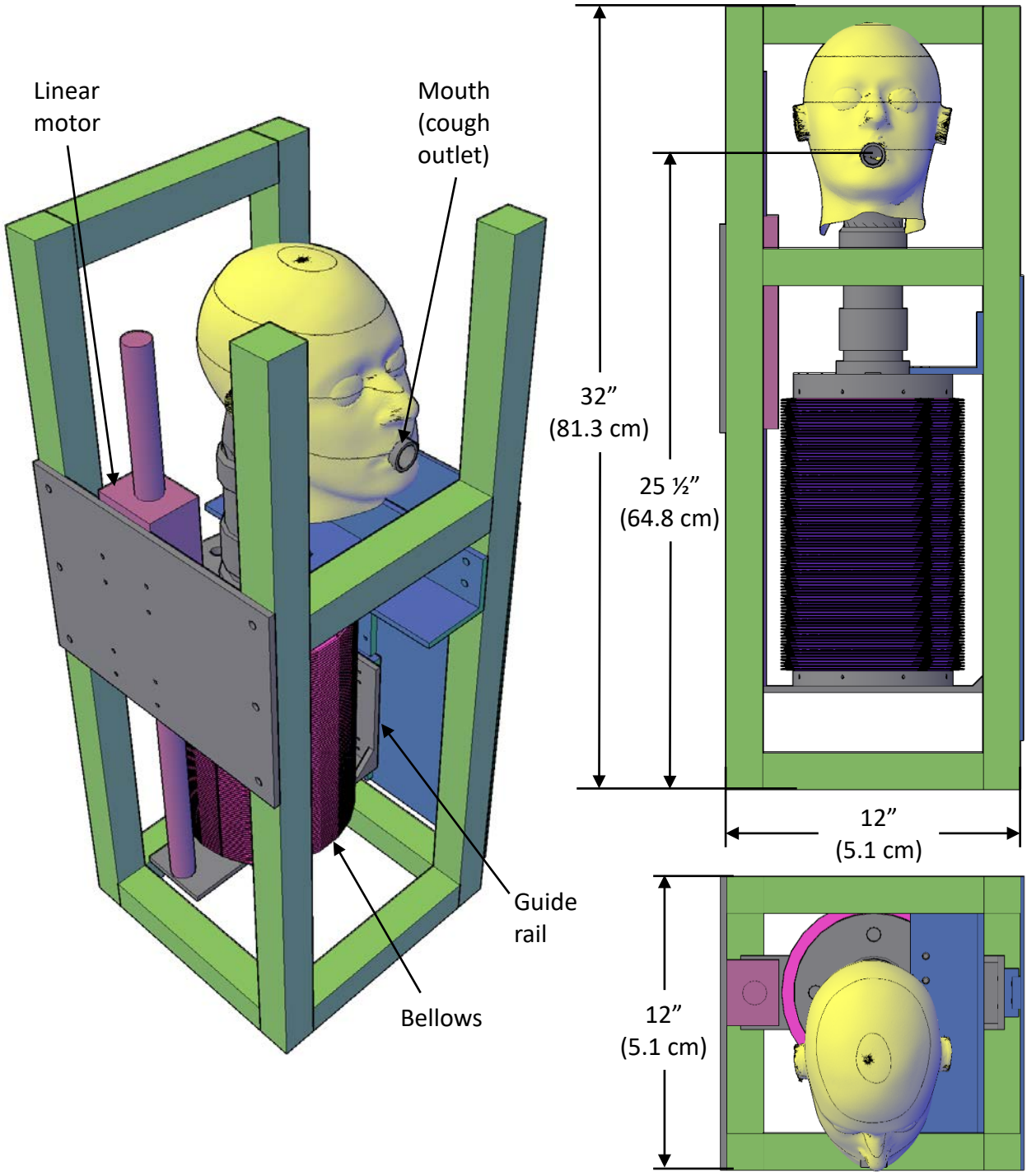

Figure S1: NIOSH cough aerosol simulator. The simulator produces a cough with a volume of 4.2 liters and a peak flow rate of 11 liters/second.

COUGH AEROSOL SIMULATOR OUTPUT

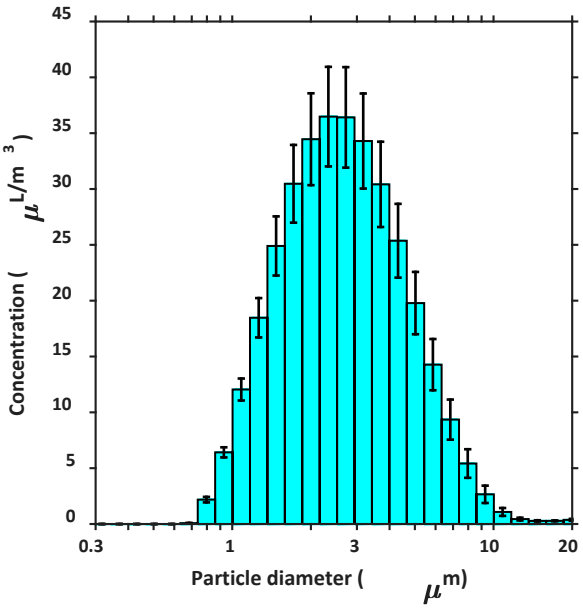

Figure S2: The size distribution of the cough aerosol generated by the simulator is shown for the 28% KCl solution with the cot angle at 30°. The histogram shows the volume concentration of the aerosol expelled by the cough simulator in each of 28 size bins for aerosol particles from 0.3 to 20 µm in diameter. At this angle, the cough aerosol had a volume geometric mean particle diameter of 2.6 µm, a geometric standard deviation of 1.7, and a total aerosol volume concentration of 202 µL/m^3 of air for particles between 0.3 and 3 µm in diameter. The size distribution of the cough aerosol output was similar at the other cot angles, but the concentration of the cough aerosol was 7% higher at 0° and 14% lower at 60° compared to 30°, as shown in Table S1 below.

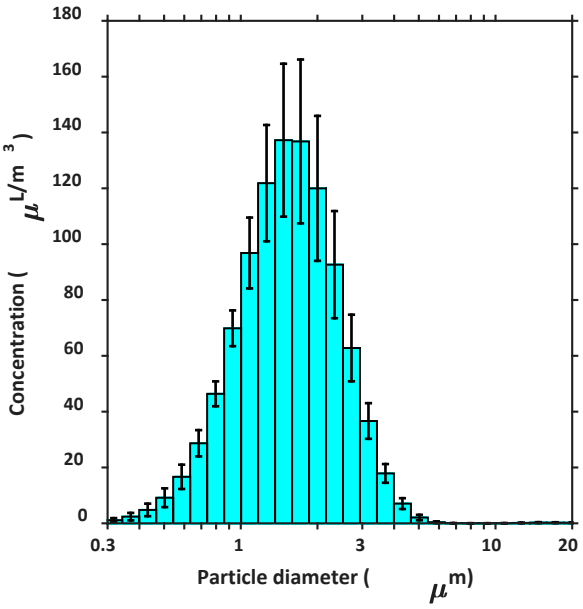

Figure S3: The cough aerosol output with the MHBSS used as a suspending media for the influenza virus had a volume geometric mean of 1.5 µm, a geometric standard deviation of 1.6, and a total aerosol volume concentration of 947 µL/m^3 of air for particles between 0.3 and 3 µm in diameter, indicating that the MHBSS cough aerosol was composed of smaller particles on average than the 28% KCl aerosol, and had a markedly higher concentration.

Table S1: Characteristics of the cough aerosol output from the NIOSH cough aerosol simulator. Results are the mean and standard deviation (in parentheses) from six trials at each angle for the 28% KCl, and twelve trials for the MHBSS.

Cot angle	*Aerosol medium*	*Volume concentration of cough aerosol (µL/m^3)*	*Volume concentration of cough aerosol between 0.3 and 3 µm (µL/m^3)*	*Volume geometric mean diameter of aerosol (µm)*	*Volume geometric standard deviation*
0°	28% KCl	376 (40)	216 (28)	2.68 (0.06)	1.76 (0.02)
30°	28% KCl	346 (40)	202 (22)	2.65 (0.06)	1.72 (0.03)
60°	28% KCl	286 (18)	173 (10)	2.58 (0.03)	1.70 (0.02)
30°	MHBSS	1013 (145)	947 (140)	1.51 (0.04)	1.59 (0.06)

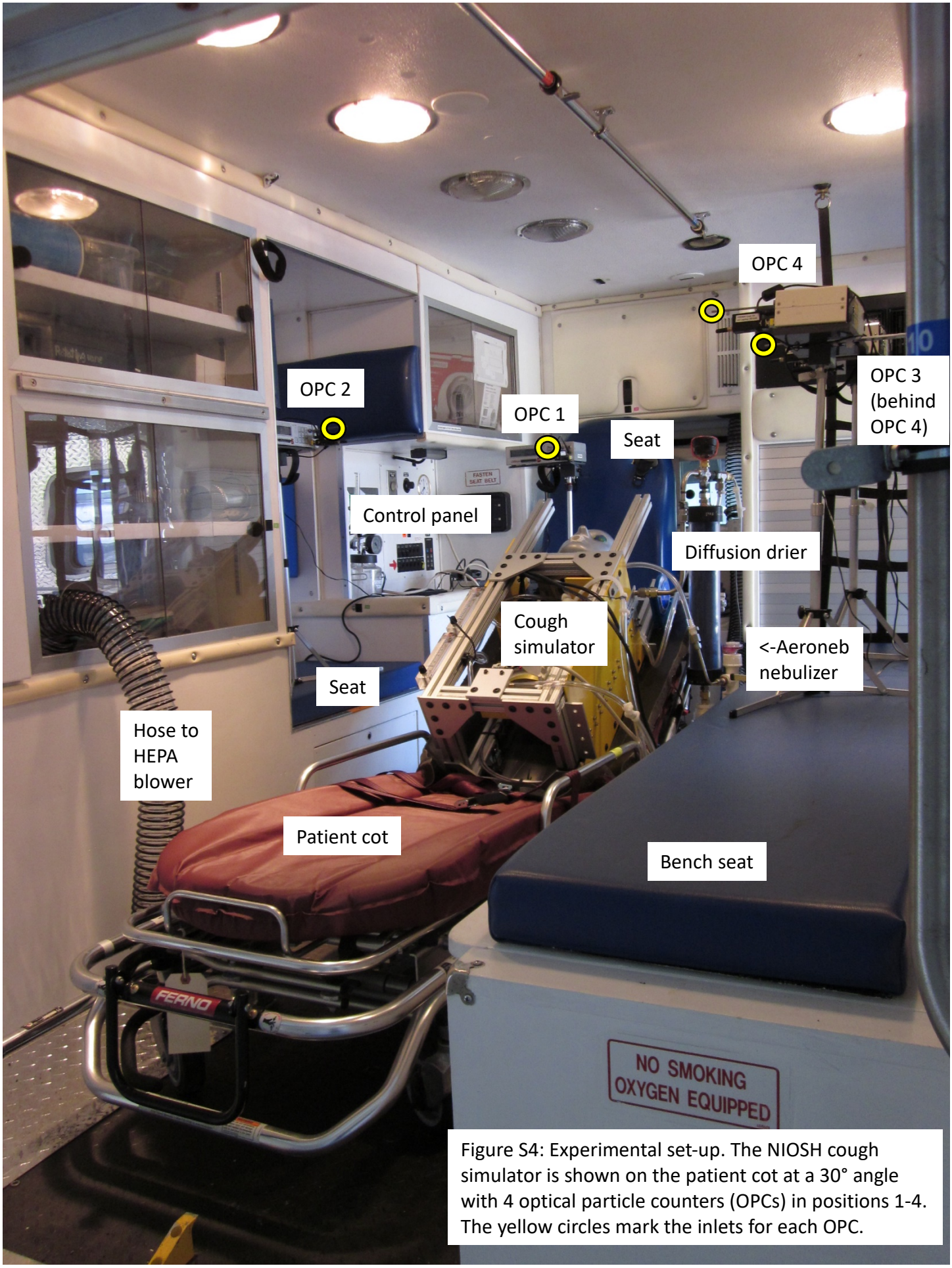

Figure S4: Experimental set-up. The NIOSH cough simulator is shown on the patient cot at a 30° angle with 4 optical particle counters (OPCs) in positions 1-4. The yellow circles mark the inlets for each OPC.

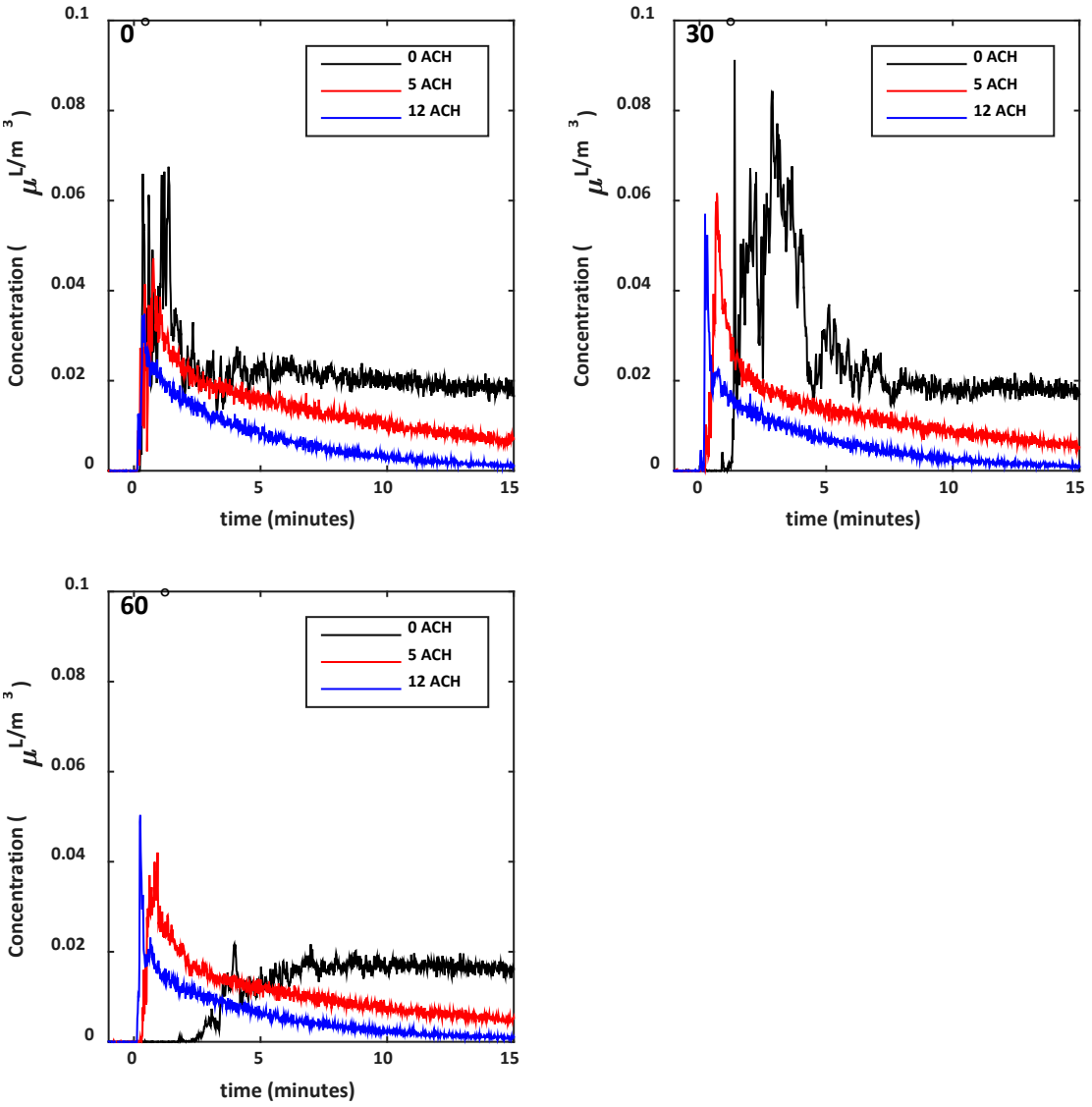

Figure S5: Aerosol volume concentration over time at position 1 with the cot at 0°, 30° and 60°. The aerosol volume concentration is the total volume of KCl aerosol particles from 0.3 to 3 µm in diameter per m3 of air. Because the output from the cough aerosol simulator changes with the cot angle, the volume concentrations at 0° were divided by 1.067 and the 60° concentrations by 0.858 to normalize them to the 30° cot angle results. ACH is compartment air changes/hour. Each line is the mean of four experiments.

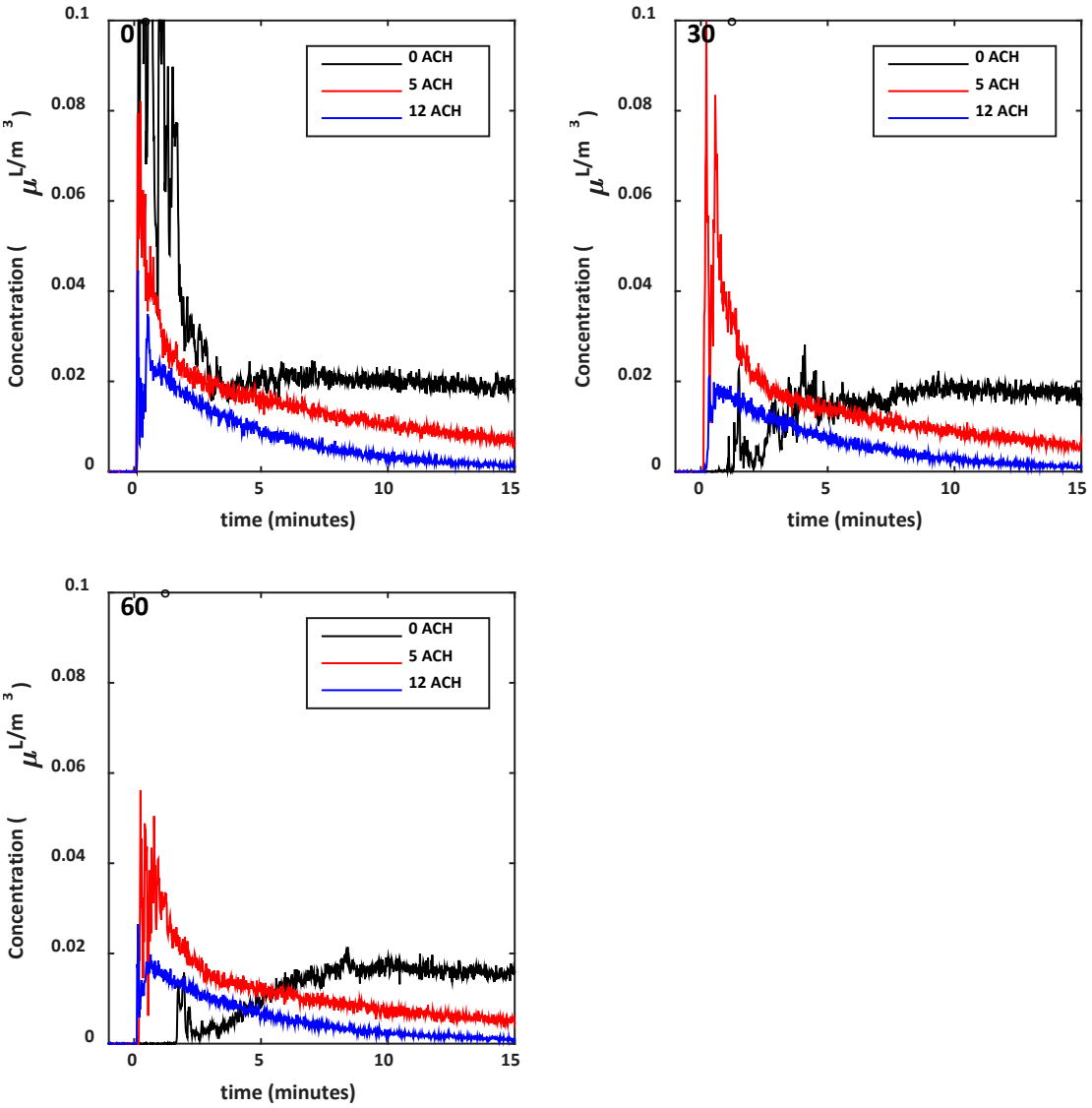

Figure S6: Aerosol volume concentration over time at position 2 with the cot at 0°, 30° and 60°.

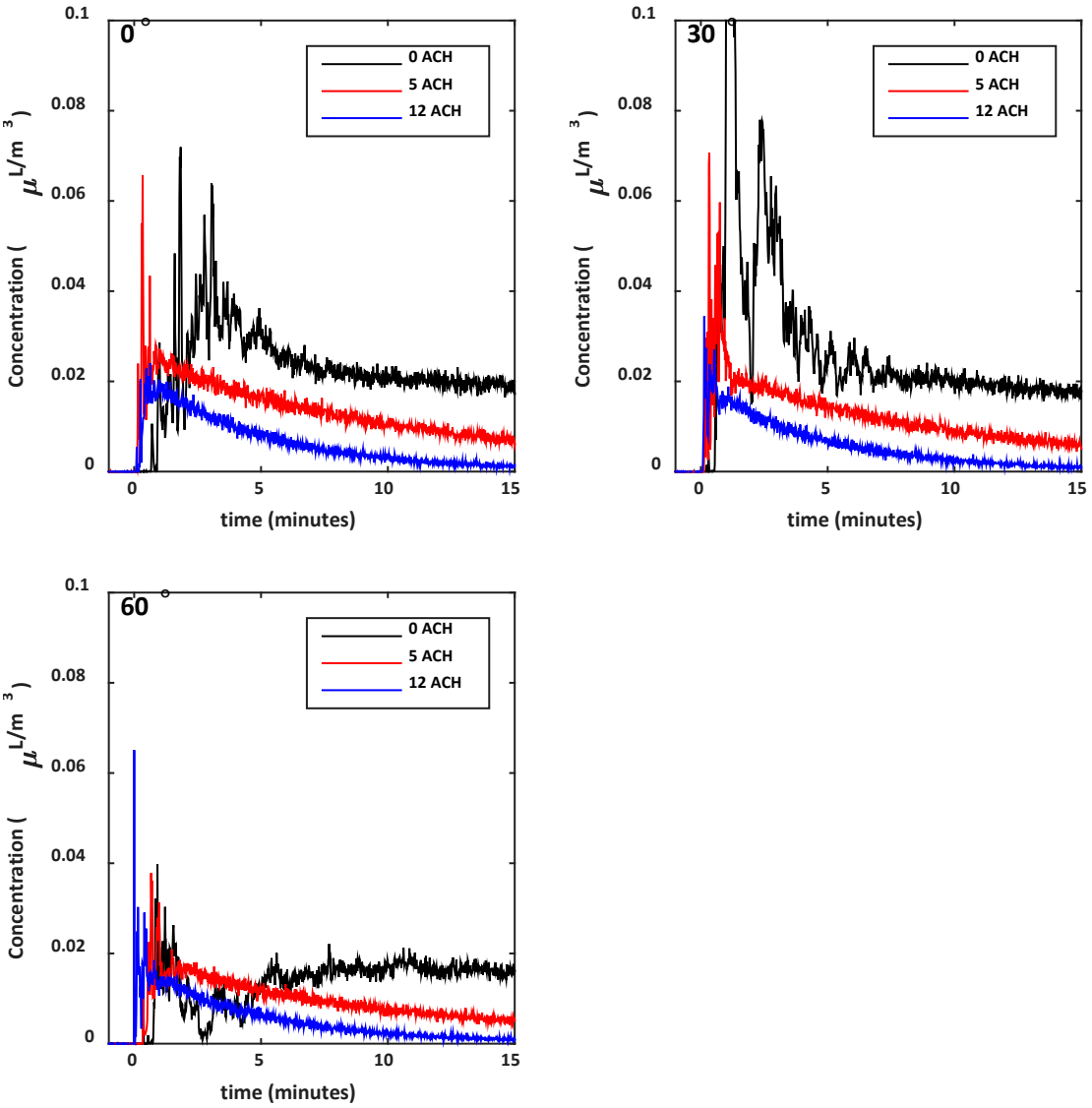

Figure S7: Aerosol volume concentration over time at position 4 with the cot at 0°, 30° and 60°.

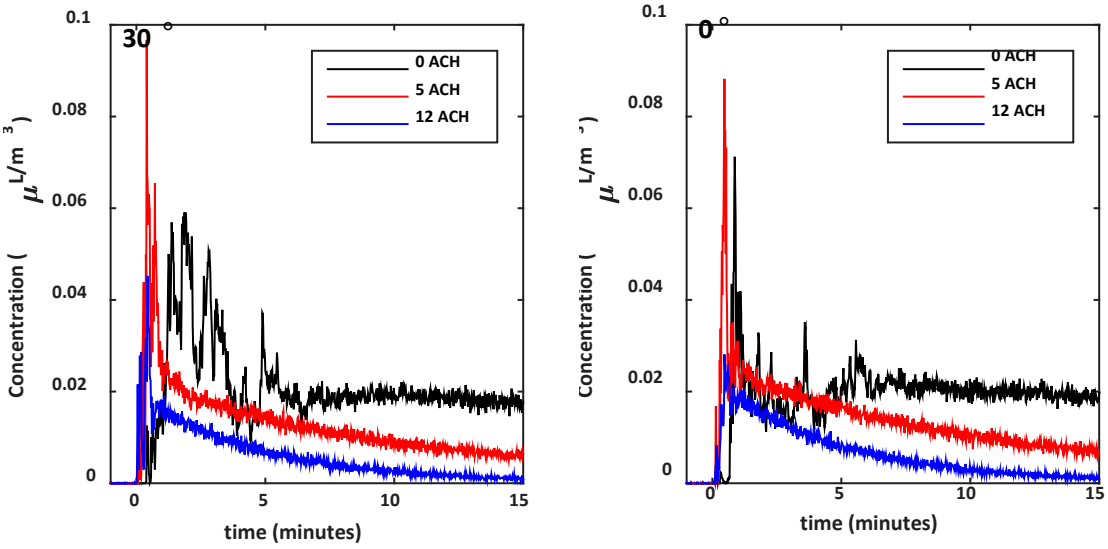

Figure S8: Aerosol volume concentration over time at position 3 with the cot at 0° and 30°.

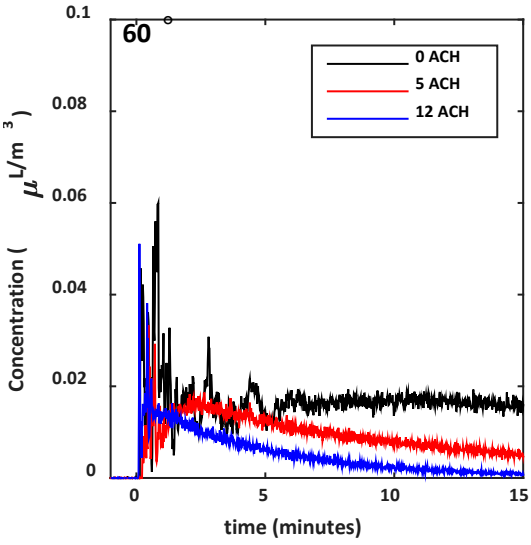

Figure S8: Aerosol volume concentration over time at position 5 with the cot at 60°.

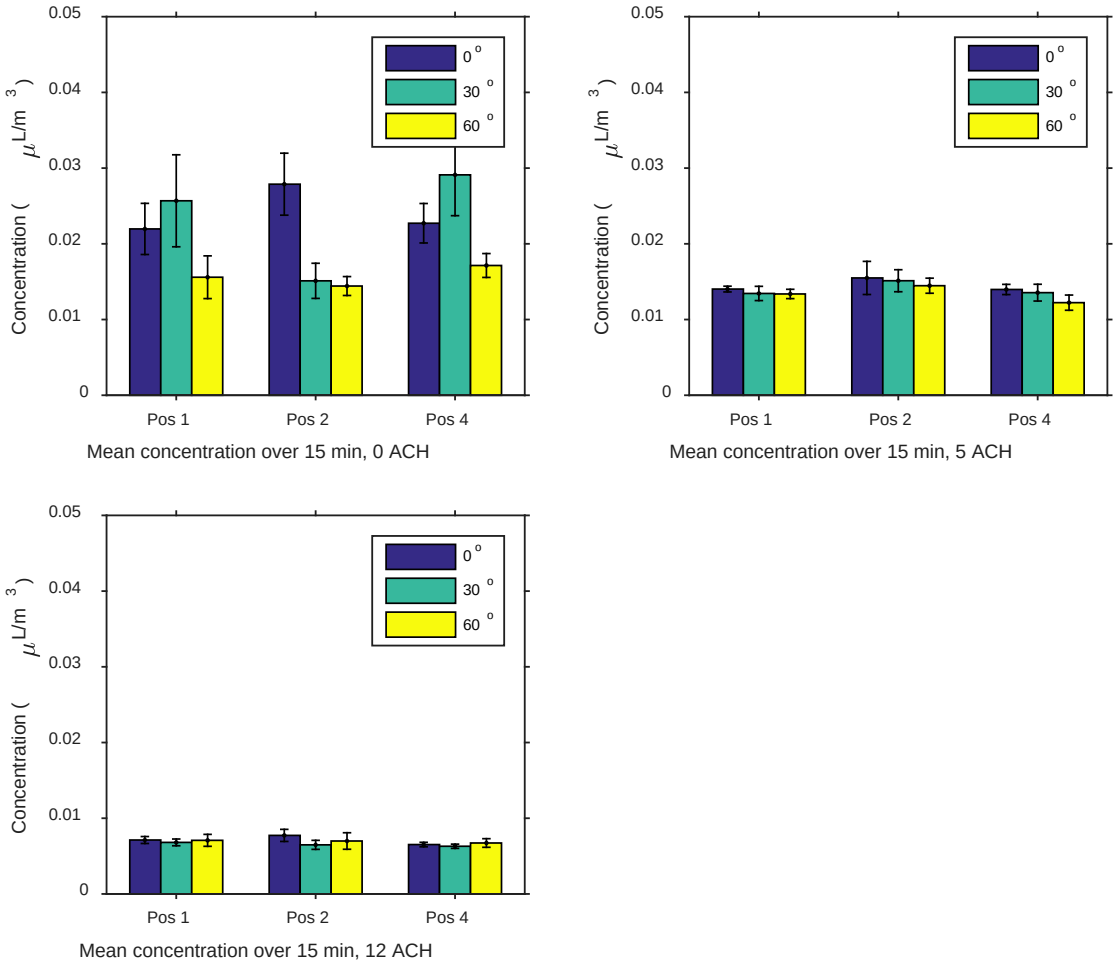

Figure S9: Mean concentration at each position and cot angle for different ACH levels. This figure shows the same data as in Figure 3, but with the groups showing the results for each cot angle rather than each ACH. Only data from positions 1, 2 and 4 are shown since those were the only positions used for all cot angles. At 0 ACH, some differences can be seen at different cot angles, but at 5 and 12 ACH the results are similar for each cot angle.

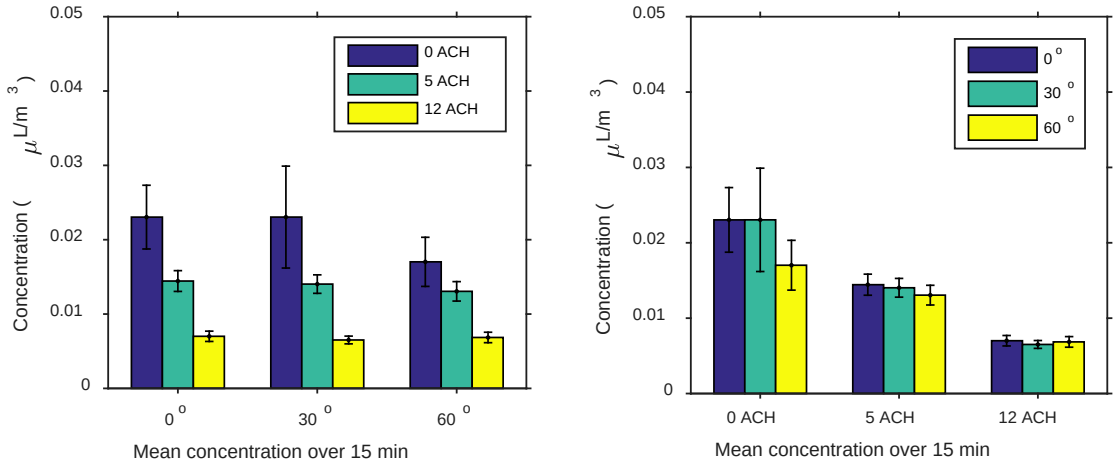

Figure S10: Mean of the concentrations at all positions combined (that is, the overall mean concentration inside the patient compartment) at each cot angle and ACH.

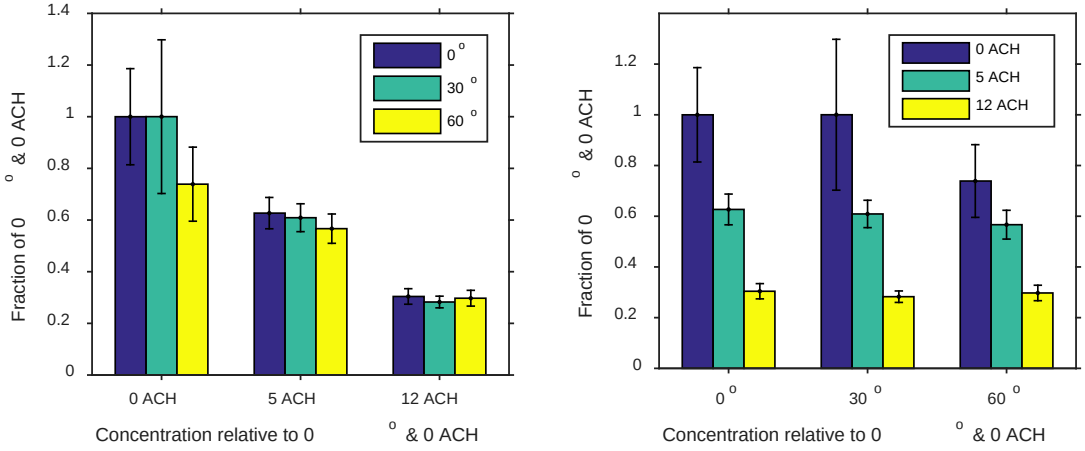

Figure S11: Overall mean concentration at each cot angle and ACH relative to the mean concentration at 0 ACH with the cot at 0°.

AEROSOL VOLUME CONCENTRATION VS. NUMBER CONCENTRATION FOR BIOAEROSOLS

In this paper, the aerosol concentration data are reported in units of volume concentration (total **volume** of aerosol particles per unit volume of air) rather than number concentration (total **number** of aerosol particles per unit volume of air). The reason is that the volume concentration provides a better description of the number of airborne microorganisms than does the number concentration. Here is an explanation.

Let us assume that we have a liquid media containing a uniform concentration of microorganisms, and that we use the media to produce an aerosol. Let us also assume that the microorganisms are small enough that we can ignore their size relative to the size of the aerosol particles. In this case, the number of microorganisms in each aerosol particle would be directly proportional to the volume of that particle, which is proportional to the cube of the particle diameter:

$$N_{microorg} = C_{microorg} V_{part} = C_{microorg} \frac{\pi}{6} {d_{part}}^3 \qquad \text{(S1)}$$

Where:

$N_{microorg}$ = number of microorganisms per particle

$C_{microorg}$ = concentration of microorganisms in suspending media, in number of microorganisms/μm^3

V_{part} = volume of particle in μm^3

d_{part} = particle diameter in μm

As an example, a 3 µm particle has a diameter 10 times larger than a 0.3 µm particle and therefore has 1000 times the volume (10^3). Thus, in this model, a 3 µm particle would contain 1000 times as many microorganisms as a 0.3 µm particle. (For simplicity, all of the calculations here are in µm and μm^3. In the paper, the aerosol volume concentrations are given in $\mu L/m^3$, where 1 µL = 10^9 μm^3).

Now suppose that our liquid media has a uniform microorganism concentration of 1000 microorganisms/μm^3 of media. Let's use this media to produce two aerosol clouds: Aerosol Cloud A contains 500 aerosol particles with a diameter of 0.306 µm in 1 m^3 of air, and Aerosol Cloud B contains 500 aerosol particles with a diameter of 3.06 µm in 1 m^3 of air. In this case, Aerosol Cloud A and Aerosol Cloud B have the same aerosol particle number concentration—500 particles/m^3 of air. However, because the volume of a 0.306 µm particle is 0.015 μm^3 while the volume of a 3 µm particle is 15 μm^3, the total volume of the aerosol particles in Aerosol Cloud A is 500 x 0.015 μm^3 = 7.5 μm^3, while the total volume of the aerosol particles in Aerosol Cloud B is 500 x 15 μm^3 = 7500 μm^3. Thus, Aerosol Cloud A has a volume concentration of 7.5 $\mu m^3/m^3$ of air, while Aerosol Cloud B has a volume concentration of 7500 $\mu m^3/m^3$ of air.

Next, let's calculate how many microorganisms are contained in each aerosol cloud. Since Aerosol Cloud A has a total particle volume of 7.5 μm^3, it contains 7.5 μm^3 x 1000 microorganisms/μm^3 = 7500 microorganisms. Since Aerosol Cloud B has a total particle volume of 7500 μm^3, it contains 7500 μm^3 x 1000 microorganisms/μm^3 = 7,500,000 microorganisms.

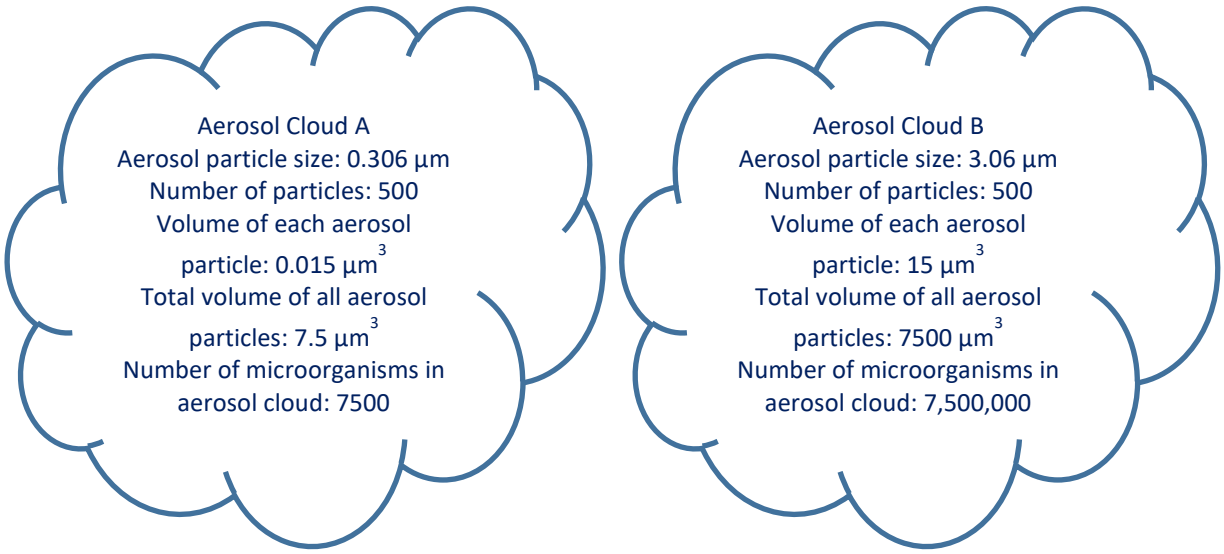

Notice the relationships between the number concentrations, volume concentrations, and number of microorganisms in each aerosol cloud. Aerosol Cloud A and Aerosol Cloud B have the same aerosol number concentration. However, the volume concentration and the number of microorganisms are both 1000 times greater for Aerosol Cloud B than for Aerosol Cloud A. Thus, the number of microorganisms is proportional to the volume concentration in the two aerosol clouds, while it is not proportional to the number concentration. This is the reason that volume concentration is used in the paper.

Equation S1 is a simplified model of the relationship between aerosol particle volume and the number of microorganisms in the particle. This relationship becomes more complex when the concentration of the microorganisms in the suspending media is low or when size of the microorganism approaches the size of the aerosol particle, because some aerosol particles will contain one or more microorganisms while others will contain none. Raabe (1968) has an analysis of the statistical distribution of microspheres in aerosol droplets that is produced when an aqueous solution of microspheres in water is aerosolized, and the principles in his analysis apply here as well. Raabe's analysis is also discussed in Chen et al. (2011).

Some researchers have experimentally examined the relationship between the number of microorganisms and aerosol particle diameter in sub-micrometer aerosols. The theoretical relationship between the number of microorganisms and particle diameter in Equation S1 above is a power-law relationship with a coefficient of 3 (that is, the number of microorganisms is proportional to d_{part}^3). Zuo et al. (2013) aerosolized four different viruses and compared particle size and count to the total number of virions for aerosol particles from 100 to 400 nm in diameter. They found that the best-fit power law coefficients ranged from 3.28 to 4.95. The authors suggest that this may be in part because the particles were separated using a differential mobility analyzer and that larger particles with multiple charges may have been inadvertently collected along with the smaller single-charged particles in each particle size bin. They also suggest that the composition of the suspending media may be a factor. Walls et al. (2016) aerosolized MS2 bacteriophage and studied particles from 45 nm to 300 nm. They found a power law coefficient of 2.64 for infectious MS2. Pan et al. (2019) aerosolized MS2 bacteriophage in three different

types of suspending media and found power law coefficients of 3.07 for total MS2 in deionized water, 2.40 in beef extract solution, and 3.44 in artificial saliva. They also presented a model showing how factors such as partitioning the virus toward the surface of the media or agglomeration of the virus could affect the power law coefficient. Thus, the experimental data support the theoretical result that the number of microorganisms in an aerosol particle is proportional to the particle volume, but suggest that other factors may play a role as well and may affect the power coefficient.

References

Chen, BT, RA Fletcher and YS Cheng (2011). Calibration of Aerosol Instruments. In: *Aerosol Measurement: Principles, Techniques, and Applications*. P. Kulkarni, P. A. Baron and K. Willeke. Hoboken, NJ, John Wiley & Sons: 449-478.

Pan, M, L Carol, JA Lednicky, A Eiguren-Fernandez, S Hering, ZH Fan and CY Wu (2019). Determination of the distribution of infectious viruses in aerosol particles using water-based condensational growth technology and a bacteriophage MS2 model. *Aerosol Sci Technol* 53(5): 583-593.

Raabe, OG (1968). The dilution of monodisperse suspensions for aerosolization. *Am Ind Hyg Assoc J* 29(5): 439-43.

Walls, HJ, DS Ensor, LA Harvey, JH Kim, RT Chartier, SV Hering, SR Spielman and GS Lewis (2016). Generation and sampling of nanoscale infectious viral aerosols. *Aerosol Sci Technol* 50(8): 802-811.

Zuo, Z, TH Kuehn, H Verma, S Kumar, SM Goyal, J Appert, PC Raynor, S Ge and DYH Pui (2013). Association of Airborne Virus Infectivity and Survivability with its Carrier Particle Size. *Aerosol Sci Technol* 47(4): 373-382.

PREDICTED VS. ACTUAL EFFECT OF VENTILATION RATE ON AEROSOL CONCENTRATION

For a simple first-order theoretical analysis of the expected effects of the ventilation system on the aerosol concentration in the patient compartment, let us assume that the air in the compartment is continuously well-mixed (that is, the aerosol concentration is the same everywhere in the compartment). Let us also assume that the losses due to particle settling are small compared to losses due to the ventilation system over the 15-minute experiment time interval for the 0.3 to 3 µm particles that we are examining.

If the compartment has an initial concentration of C_I and an air change rate of k, then the concentration at time t is

$$C(t) = C_I\, e^{-kt}$$

In our case, we will express t in hours and k in air changes/hour. For t = 0.25 hours (15 minutes) and k = 5 ACH, we find that $C(t)/C_I = 0.287$. This means that the filtration system would be expected to reduce the particle concentration at all locations to 29% of the initial concentration after 15 minutes. Similarly, if t = 0.25 and k = 12 ACH, then $C(t)/C_I = 0.050$, indicating that with 12 air changes/hour, we would expect to see the concentration fall to 5% of the initial value after 15 minutes.

The mean aerosol concentration C_{mean} to which the worker is exposed over time interval T is found by integrating C(t) over T:

$$C_{mean} = \frac{\int_0^T C_I\, e^{-kt}}{T}$$

$$C_{mean} = \frac{C_I}{T} \int_0^T e^{-kt}$$

$$C_{mean} = -\frac{C_I}{kT} \left[e^{-kT} - e^{-k0}\right]$$

$$C_{mean} = \frac{C_I}{kT} \left[e^{-k0} - e^{-kT}\right]$$

$$C_{mean} = \frac{C_I}{kT} \left[1 - e^{-kT}\right]$$

If k = 5 ACH and T = 0.25 hours, then kT = 1.25 and C_{mean} = 0.571 C_I.

If k = 12 ACH and T = 0.25 hours, then kT = 3 and C_{mean} = 0.317 C_I.

Now let us compare these calculations to the experimental results. If we average the experimental volume concentration results from the OPCs for all positions and cot angles for each air change rate, we find that the mean concentration at 5 ACH is 66% of the 0 ACH mean (SD 19%), and the mean concentration at 12 ACH is 32% of the 0 ACH mean (SD 9%), which is close to the predicted results. Similarly, if we average the influenza test results for both positions, we find that the mean concentration at 5 ACH is 65% of the 0 ACH mean (SD 25%), and the mean concentration at 12 ACH is 36% of the 0 ACH mean (SD 20%), which again is close to the predicted results.

A discussion of the measurement of air change rates and concentrations using a variety of techniques can be found in: Grieve, PW (1991). “Measuring Ventilation Using Tracer-Gases”. Bruel & Kjaer, Denmark, available online at https://innova.lumasenseinc.com/manuals/booklets/.

EXPERIMENTAL DATA

Experiments with coughs produced using 28% KCl in the Collison nebulizer
Each experimental condition (cot angle and air changes/hour (ACH)) was repeated 4 times with the optical particle counters rotated among the positions.
Note that, when the cot angle was 0 or 30 degrees, positions 1-4 were used
and when the cot angle was 60 degrees, positions 1-2 and 4-5 were used.
The normalization factor accounts for differences in aerosol output from the cough simulator at different cot angles

Experiment #	Instrument S/N	Instrument Position	Cot Angle	Air changes/hour ACH	Mean Aerosol Concentration (uL/liter of air)	Normalization Factor	Normalized mean concentration (uL/m^3)
AKC001	34	1	0	0	27.81433905	1.067311205	2.61E-02
AKC001	45	2	0	0	29.05523006	1.067311205	2.72E-02
AKC001	44	3	0	0	22.47963878	1.067311205	2.11E-02
AKC001	24	4	0	0	23.51703992	1.067311205	2.20E-02
AKC002	45	1	0	0	19.06686899	1.067311205	1.79E-02
AKC002	44	2	0	0	24.25374112	1.067311205	2.27E-02
AKC002	24	3	0	0	16.82050396	1.067311205	1.58E-02
AKC002	34	4	0	0	21.69343442	1.067311205	2.03E-02
AKC003	44	1	0	0	22.85325601	1.067311205	2.14E-02
AKC003	24	2	0	0	34.7637828	1.067311205	3.26E-02
AKC003	34	3	0	0	20.49301867	1.067311205	1.92E-02
AKC003	45	4	0	0	28.20951045	1.067311205	2.64E-02
AKC004	24	1	0	0	24.04826253	1.067311205	2.25E-02
AKC004	34	2	0	0	30.9428124	1.067311205	2.90E-02
AKC004	45	3	0	0	23.85346761	1.067311205	2.23E-02
AKC004	44	4	0	0	23.5762496	1.067311205	2.21E-02

AKC005	34	1	0	5	14.65969309	1.067311205	1.37E-02
AKC005	45	2	0	5	14.54603951	1.067311205	1.36E-02
AKC005	44	3	0	5	12.96223115	1.067311205	1.21E-02
AKC005	24	4	0	5	14.6814251	1.067311205	1.38E-02
AKC006	45	1	0	5	15.03493717	1.067311205	1.41E-02
AKC006	44	2	0	5	14.87713238	1.067311205	1.39E-02
AKC006	24	3	0	5	16.6677227	1.067311205	1.56E-02
AKC006	34	4	0	5	15.73662827	1.067311205	1.47E-02
AKC007	44	1	0	5	14.66330555	1.067311205	1.37E-02
AKC007	24	2	0	5	19.57899554	1.067311205	1.83E-02
AKC007	34	3	0	5	16.10422716	1.067311205	1.51E-02
AKC007	45	4	0	5	14.04626472	1.067311205	1.32E-02
AKC008	24	1	0	5	15.51730335	1.067311205	1.45E-02
AKC008	34	2	0	5	17.14429777	1.067311205	1.61E-02
AKC008	45	3	0	5	15.21468129	1.067311205	1.43E-02
AKC008	44	4	0	5	15.17917794	1.067311205	1.42E-02
AKC009	34	1	0	12	7.63386722	1.067311205	7.15E-03
AKC009	45	2	0	12	7.54581966	1.067311205	7.07E-03
AKC009	44	3	0	12	6.35240257	1.067311205	5.95E-03
AKC009	24	4	0	12	7.25564682	1.067311205	6.80E-03
AKC010	45	1	0	12	7.03504601	1.067311205	6.59E-03
AKC010	44	2	0	12	7.48774221	1.067311205	7.02E-03
AKC010	24	3	0	12	7.31132609	1.067311205	6.85E-03
AKC010	34	4	0	12	7.1853861	1.067311205	6.73E-03
AKC011	44	1	0	12	7.52148615	1.067311205	7.05E-03
AKC011	24	2	0	12	9.0301219	1.067311205	8.46E-03
AKC011	34	3	0	12	7.62726495	1.067311205	7.15E-03
AKC011	45	4	0	12	6.83429334	1.067311205	6.40E-03
AKC012	24	1	0	12	8.22596422	1.067311205	7.71E-03
AKC012	34	2	0	12	8.9516751	1.067311205	8.39E-03

AKC012	45	3	0	12	7.08875017	1.067311205	6.64E-03
AKC012	44	4	0	12	6.57810422	1.067311205	6.16E-03
AKC013	34	1	30	0	32.81387758	1	3.28E-02
AKC013	45	2	30	0	13.7098732	1	1.37E-02
AKC013	44	3	30	0	25.99427027	1	2.60E-02
AKC013	24	4	30	0	34.44620891	1	3.44E-02
AKC014	45	1	30	0	25.88061219	1	2.59E-02
AKC014	44	2	30	0	13.02543807	1	1.30E-02
AKC014	24	3	30	0	26.0699938	1	2.61E-02
AKC014	34	4	30	0	30.61530407	1	3.06E-02
AKC015	44	1	30	0	17.9586727	1	1.80E-02
AKC015	24	2	30	0	15.48351225	1	1.55E-02
AKC015	34	3	30	0	20.1183869	1	2.01E-02
AKC015	45	4	30	0	21.62415974	1	2.16E-02
AKC016	24	1	30	0	26.08145987	1	2.61E-02
AKC016	34	2	30	0	18.2253558	1	1.82E-02
AKC016	45	3	30	0	16.91844233	1	1.69E-02
AKC016	44	4	30	0	29.74713069	1	2.97E-02
AKC017	34	1	30	5	13.91952039	1	1.39E-02
AKC017	45	2	30	5	13.67705654	1	1.37E-02
AKC017	44	3	30	5	12.49818939	1	1.25E-02
AKC017	24	4	30	5	15.20207896	1	1.52E-02
AKC018	45	1	30	5	12.44225782	1	1.24E-02
AKC018	44	2	30	5	14.28404608	1	1.43E-02
AKC018	24	3	30	5	14.02944822	1	1.40E-02
AKC018	34	4	30	5	13.16574038	1	1.32E-02
AKC019	44	1	30	5	12.90461722	1	1.29E-02
AKC019	24	2	30	5	15.58895974	1	1.56E-02
AKC019	34	3	30	5	14.87990456	1	1.49E-02
AKC019	45	4	30	5	12.86682163	1	1.29E-02

AKC020	24	1	30	5	14.50989875	1	1.45E-02
AKC020	34	2	30	5	16.94864042	1	1.69E-02
AKC020	45	3	30	5	14.60310127	1	1.46E-02
AKC020	44	4	30	5	12.96657409	1	1.30E-02
AKC021	34	1	30	12	6.72830693	1	6.73E-03
AKC021	45	2	30	12	5.83963477	1	5.84E-03
AKC021	44	3	30	12	5.49492014	1	5.49E-03
AKC021	24	4	30	12	6.21397833	1	6.21E-03
AKC022	45	1	30	12	6.57704635	1	6.58E-03
AKC022	44	2	30	12	6.13429489	1	6.13E-03
AKC022	24	3	30	12	6.93192121	1	6.93E-03
AKC022	34	4	30	12	6.71001719	1	6.71E-03
AKC023	44	1	30	12	6.47176939	1	6.47E-03
AKC023	24	2	30	12	6.87332936	1	6.87E-03
AKC023	34	3	30	12	7.11919948	1	7.12E-03
AKC023	45	4	30	12	6.07023453	1	6.07E-03
AKC024	24	1	30	12	7.45994928	1	7.46E-03
AKC024	34	2	30	12	7.09498985	1	7.09E-03
AKC024	45	3	30	12	6.28048896	1	6.28E-03
AKC024	44	4	30	12	6.20499556	1	6.20E-03
AKC025	34	1	60	0	15.43393363	0.85816518	1.80E-02
AKC025	45	2	60	0	11.6495921	0.85816518	1.36E-02
AKC025	44	4	60	0	14.66617091	0.85816518	1.71E-02
AKC025	24	5	60	0	18.42475527	0.85816518	2.15E-02
AKC026	45	1	60	0	12.55257725	0.85816518	1.46E-02
AKC026	44	2	60	0	11.33243998	0.85816518	1.32E-02
AKC026	24	4	60	0	13.22924769	0.85816518	1.54E-02
AKC026	34	5	60	0	16.91428718	0.85816518	1.97E-02
AKC027	44	1	60	0	10.31963729	0.85816518	1.20E-02
AKC027	24	2	60	0	12.9255502	0.85816518	1.51E-02

AKC027	34	4	60	0	14.42738332	0.85816518	1.68E-02
AKC027	45	5	60	0	15.00327965	0.85816518	1.75E-02
AKC028	24	1	60	0	15.20187483	0.85816518	1.77E-02
AKC028	34	2	60	0	13.6095889	0.85816518	1.59E-02
AKC028	45	4	60	0	16.5039968	0.85816518	1.92E-02
AKC028	44	5	60	0	21.5330893	0.85816518	2.51E-02
AKC029	34	1	60	5	12.15310381	0.85816518	1.42E-02
AKC029	45	2	60	5	13.13541929	0.85816518	1.53E-02
AKC029	44	4	60	5	9.98964581	0.85816518	1.16E-02
AKC029	24	5	60	5	11.15227203	0.85816518	1.30E-02
AKC030	45	1	60	5	11.32856535	0.85816518	1.32E-02
AKC030	44	2	60	5	12.33085766	0.85816518	1.44E-02
AKC030	24	4	60	5	11.19967523	0.85816518	1.31E-02
AKC030	34	5	60	5	11.27098024	0.85816518	1.31E-02
AKC031	44	1	60	5	10.88240059	0.85816518	1.27E-02
AKC031	24	2	60	5	12.95364507	0.85816518	1.51E-02
AKC031	34	4	60	5	11.24787646	0.85816518	1.31E-02
AKC031	45	5	60	5	10.1258415	0.85816518	1.18E-02
AKC032	24	1	60	5	11.55519149	0.85816518	1.35E-02
AKC032	34	2	60	5	11.24344334	0.85816518	1.31E-02
AKC032	45	4	60	5	9.54096993	0.85816518	1.11E-02
AKC032	44	5	60	5	9.13903425	0.85816518	1.06E-02
AKC033	34	1	60	12	6.36247142	0.85816518	7.41E-03
AKC033	45	2	60	12	5.79163378	0.85816518	6.75E-03
AKC033	44	4	60	12	5.3470014	0.85816518	6.23E-03
AKC033	24	5	60	12	5.83521359	0.85816518	6.80E-03
AKC034	45	1	60	12	5.09747421	0.85816518	5.94E-03
AKC034	44	2	60	12	4.81218723	0.85816518	5.61E-03
AKC034	24	4	60	12	5.46984972	0.85816518	6.37E-03
AKC034	34	5	60	12	5.20238239	0.85816518	6.06E-03

AKC035	44	1	60	12	6.20622436	0.85816518	7.23E-03
AKC035	24	2	60	12	7.00944441	0.85816518	8.17E-03
AKC035	34	4	60	12	6.43305556	0.85816518	7.50E-03
AKC035	45	5	60	12	5.73066747	0.85816518	6.68E-03
AKC036	24	1	60	12	6.63970419	0.85816518	7.74E-03
AKC036	34	2	60	12	6.39297097	0.85816518	7.45E-03
AKC036	45	4	60	12	5.85521322	0.85816518	6.82E-03
AKC036	44	5	60	12	5.8832601	0.85816518	6.86E-03

Experiments with coughs produced using influenza virus in MHBSS with Aeroneb nebulizer
In these experiments, the cough simulator coughed an aerosol containing influenza virus into the compartment and the aerosolized virus was collected at two positons using SKC BioSamplers for 15 minutes after the cough.
M1 copies is the number copies of the influenza M1 gene detected in the sample by PCR

	Volume of air collected (m^3)		0.1875		
Experiment #	Patient cot angle	ACH	Position	M1 copies	M1 copies/m^3 air
AIC001	30°	0	P1	5.87E+04	3.13E+05
AIC001	30°	0	P4	4.90E+04	2.61E+05
AIC002	30°	0	P1	5.72E+04	3.05E+05
AIC002	30°	0	P4	6.70E+04	3.58E+05
AIC003	30°	0	P1	7.08E+04	3.78E+05
AIC003	30°	0	P4	8.94E+04	4.77E+05
AIC004	30°	5	P1	4.65E+04	2.48E+05
AIC004	30°	5	P4	2.23E+04	1.19E+05
AIC005	30°	5	P1	5.45E+04	2.91E+05
AIC005	30°	5	P4	4.68E+04	2.50E+05
AIC010	30°	5	P1	3.08E+04	1.65E+05
AIC010	30°	5	P4	5.43E+04	2.90E+05
AIC007	30°	12	P1	2.93E+04	1.56E+05
AIC007	30°	12	P4	1.70E+04	9.04E+04
AIC008	30°	12	P1	2.34E+04	1.25E+05
AIC008	30°	12	P4	2.25E+04	1.20E+05
AIC009	30°	12	P1	2.71E+04	1.45E+05
AIC009	30°	12	P4	2.05E+04	1.09E+05

SAS Analysis of experimental data

Results for Position 1:

The Mixed Procedure
Model Information

Data Set	WORK.NEW
Dependent Variable	logConc
Covariance Structure	Diagonal
Estimation Method	REML
Residual Variance Method	Profile
Fixed Effects SE Method	Model-Based
Degrees of Freedom Method	Residual

Class Level Information

Class	Levels	Values
ACH	3	0 5 12
Cot_Angle	3	0 30 60
Position	1	1

Dimensions

Covariance Parameters	1
Columns in X	16
Columns in Z	0
Subjects	1
Max Obs per Subject	36

Number of Observations

Number of Observations Read	36
Number of Observations Used	36
Number of Observations Not Used	0

Covariance Parameter Estimates

Cov Parm	Estimate
Residual	0.01688

Fit Statistics

-2 Res Log Likelihood	-21.1
AIC (Smaller is Better)	-19.1
AICC (Smaller is Better)	-18.9
BIC (Smaller is Better)	-17.8

The SAS System

The Mixed Procedure

Type 3 Tests of Fixed Effects

Effect	Num DF	Den DF	F Value	Pr > F
Cot_Angle	2	27	4.96	0.0147
ACH	2	27	207.15	<.0001
ACH*Cot_Angle	4	27	5.20	0.0031

Least Squares Means

Effect	ACH	Cot_Angle	Estimate	Standard Error	DF	t Value	Pr > |t|	Alpha
ACH*Cot_Angle	0	0	-9.1351	0.06496	27	-140.63	<.0001	0.05
ACH*Cot_Angle	0	30	-8.9922	0.06496	27	-138.43	<.0001	0.05
ACH*Cot_Angle	0	60	-9.4822	0.06496	27	-145.98	<.0001	0.05
ACH*Cot_Angle	5	0	-9.5751	0.06496	27	-147.41	<.0001	0.05
ACH*Cot_Angle	5	30	-9.6189	0.06496	27	-148.08	<.0001	0.05
ACH*Cot_Angle	5	60	-9.6229	0.06496	27	-148.14	<.0001	0.05
ACH*Cot_Angle	12	0	-10.2536	0.06496	27	-157.85	<.0001	0.05
ACH*Cot_Angle	12	30	-10.2989	0.06496	27	-158.55	<.0001	0.05
ACH*Cot_Angle	12	60	-10.2632	0.06496	27	-158.00	<.0001	0.05

The SAS System

The Mixed Procedure

Differences of Least Squares Means

Effect	ACH	Cot_Angle	ACH	Cot_Angle	Adjustment	Adj P	Alpha	Lower	Upper
ACH*Cot_Angle	0	0	0	30	Tukey	0.8194	0.05	-0.3314	0.04560
ACH*Cot_Angle	0	0	0	60	Tukey	0.0192	0.05	0.1586	0.5356
ACH*Cot_Angle	0	0	5	0	Tukey	0.0015	0.05	0.2515	0.6285
ACH*Cot_Angle	0	0	5	30	Tukey	0.0004	0.05	0.2953	0.6723

ACH*Cot_Angle	0	0	5	60	Tukey	0.0004	0.05	0.2993	0.6763
ACH*Cot_Angle	0	0	12	0	Tukey	<.0001	0.05	0.9300	1.3070
ACH*Cot_Angle	0	0	12	30	Tukey	<.0001	0.05	0.9753	1.3523
ACH*Cot_Angle	0	0	12	60	Tukey	<.0001	0.05	0.9396	1.3166
ACH*Cot_Angle	0	30	0	60	Tukey	0.0004	0.05	0.3015	0.6785
ACH*Cot_Angle	0	30	5	0	Tukey	<.0001	0.05	0.3944	0.7713
ACH*Cot_Angle	0	30	5	30	Tukey	<.0001	0.05	0.4382	0.8152
ACH*Cot_Angle	0	30	5	60	Tukey	<.0001	0.05	0.4422	0.8191
ACH*Cot_Angle	0	30	12	0	Tukey	<.0001	0.05	1.0729	1.4499
ACH*Cot_Angle	0	30	12	30	Tukey	<.0001	0.05	1.1182	1.4952
ACH*Cot_Angle	0	30	12	60	Tukey	<.0001	0.05	1.0825	1.4595
ACH*Cot_Angle	0	60	5	0	Tukey	0.9814	0.05	-0.09559	0.2814
ACH*Cot_Angle	0	60	5	30	Tukey	0.8511	0.05	-0.05174	0.3252
ACH*Cot_Angle	0	60	5	60	Tukey	0.8311	0.05	-0.04780	0.3292
ACH*Cot_Angle	0	60	12	0	Tukey	<.0001	0.05	0.5830	0.9599
ACH*Cot_Angle	0	60	12	30	Tukey	<.0001	0.05	0.6282	1.0052
ACH*Cot_Angle	0	60	12	60	Tukey	<.0001	0.05	0.5926	0.9695
ACH*Cot_Angle	5	0	5	30	Tukey	0.9999	0.05	-0.1446	0.2323
ACH*Cot_Angle	5	0	5	60	Tukey	0.9998	0.05	-0.1407	0.2363
ACH*Cot_Angle	5	0	12	0	Tukey	<.0001	0.05	0.4901	0.8670
ACH*Cot_Angle	5	0	12	30	Tukey	<.0001	0.05	0.5353	0.9123
ACH*Cot_Angle	5	0	12	60	Tukey	<.0001	0.05	0.4997	0.8766
ACH*Cot_Angle	5	30	5	60	Tukey	1.0000	0.05	-0.1845	0.1924
ACH*Cot_Angle	5	30	12	0	Tukey	<.0001	0.05	0.4462	0.8232
ACH*Cot_Angle	5	30	12	30	Tukey	<.0001	0.05	0.4915	0.8685
ACH*Cot_Angle	5	30	12	60	Tukey	<.0001	0.05	0.4558	0.8328
ACH*Cot_Angle	5	60	12	0	Tukey	<.0001	0.05	0.4423	0.8192
ACH*Cot_Angle	5	60	12	30	Tukey	<.0001	0.05	0.4875	0.8645
ACH*Cot_Angle	5	60	12	60	Tukey	<.0001	0.05	0.4519	0.8288
ACH*Cot_Angle	12	0	12	30	Tukey	0.9999	0.05	-0.1432	0.2338
ACH*Cot_Angle	12	0	12	60	Tukey	1.0000	0.05	-0.1789	0.1981
ACH*Cot_Angle	12	30	12	60	Tukey	1.0000	0.05	-0.2242	0.1528

Differences of Least Squares Means

Effect	ACH	Cot_Angle	ACH	Cot_Angle	Adj Lower	Adj Upper
ACH*Cot_Angle	0	0	0	30	-0.4520	0.1662
ACH*Cot_Angle	0	0	0	60	0.03798	0.6562
ACH*Cot_Angle	0	0	5	0	0.1309	0.7491
ACH*Cot_Angle	0	0	5	30	0.1747	0.7929
ACH*Cot_Angle	0	0	5	60	0.1787	0.7969

ACH*Cot_Angle	0	0	12	0	0.8094	1.4276
ACH*Cot_Angle	0	0	12	30	0.8547	1.4729
ACH*Cot_Angle	0	0	12	60	0.8190	1.4372
ACH*Cot_Angle	0	30	0	60	0.1809	0.7991
ACH*Cot_Angle	0	30	5	0	0.2738	0.8920
ACH*Cot_Angle	0	30	5	30	0.3176	0.9358
ACH*Cot_Angle	0	30	5	60	0.3216	0.9397
ACH*Cot_Angle	0	30	12	0	0.9523	1.5705
ACH*Cot_Angle	0	30	12	30	0.9976	1.6158
ACH*Cot_Angle	0	30	12	60	0.9619	1.5801
ACH*Cot_Angle	0	60	5	0	-0.2162	0.4020
ACH*Cot_Angle	0	60	5	30	-0.1723	0.4458
ACH*Cot_Angle	0	60	5	60	-0.1684	0.4498
ACH*Cot_Angle	0	60	12	0	0.4624	1.0805
ACH*Cot_Angle	0	60	12	30	0.5076	1.1258
ACH*Cot_Angle	0	60	12	60	0.4720	1.0901
ACH*Cot_Angle	5	0	5	30	-0.2652	0.3529
ACH*Cot_Angle	5	0	5	60	-0.2613	0.3569
ACH*Cot_Angle	5	0	12	0	0.3695	0.9876
ACH*Cot_Angle	5	0	12	30	0.4147	1.0329
ACH*Cot_Angle	5	0	12	60	0.3791	0.9972
ACH*Cot_Angle	5	30	5	60	-0.3051	0.3130
ACH*Cot_Angle	5	30	12	0	0.3256	0.9438
ACH*Cot_Angle	5	30	12	30	0.3709	0.9891
ACH*Cot_Angle	5	30	12	60	0.3352	0.9534
ACH*Cot_Angle	5	60	12	0	0.3217	0.9399
ACH*Cot_Angle	5	60	12	30	0.3669	0.9851
ACH*Cot_Angle	5	60	12	60	0.3313	0.9494
ACH*Cot_Angle	12	0	12	30	-0.2638	0.3544
ACH*Cot_Angle	12	0	12	60	-0.2995	0.3187
ACH*Cot_Angle	12	30	12	60	-0.3448	0.2734

Results for Position 2:

The Mixed Procedure

Model Information

Data Set	WORK.NEW
Dependent Variable	logConc
Covariance Structure	Diagonal
Estimation Method	REML
Residual Variance Method	Profile
Fixed Effects SE Method	Model-Based
Degrees of Freedom Method	Residual

Class Level Information

Class	Levels	Values
ACH	3	0 5 12
Cot_Angle	3	0 30 60
Position	1	2

Dimensions

Covariance Parameters	1
Columns in X	16
Columns in Z	0
Subjects	1
Max Obs per Subject	36

Number of Observations

Number of Observations Read	36
Number of Observations Used	36
Number of Observations Not Used	0

Covariance Parameter Estimates

Cov Parm	Estimate
Residual	0.01451

Fit Statistics

-2 Res Log Likelihood	-25.2
AIC (Smaller is Better)	-23.2
AICC (Smaller is Better)	-23.0
BIC (Smaller is Better)	-21.9

The SAS System
The Mixed Procedure

Type 3 Tests of Fixed Effects

Effect	Num DF	Den DF	F Value	Pr > F
Cot_Angle	2	27	20.36	<.0001
ACH	2	27	208.51	<.0001
ACH*Cot_Angle	4	27	9.50	<.0001

Least Squares Means

Effect	ACH	Cot_Angle	Estimate	Standard Error	DF	t Value	Pr > |t|	Alpha
ACH*Cot_Angle	0	0	-8.8962	0.06023	27	-147.70	<.0001	0.05
ACH*Cot_Angle	0	30	-9.5087	0.06023	27	-157.87	<.0001	0.05
ACH*Cot_Angle	0	60	-9.5494	0.06023	27	-158.55	<.0001	0.05
ACH*Cot_Angle	5	0	-9.4825	0.06023	27	-157.44	<.0001	0.05
ACH*Cot_Angle	5	30	-9.5027	0.06023	27	-157.77	<.0001	0.05
ACH*Cot_Angle	5	60	-9.5455	0.06023	27	-158.48	<.0001	0.05
ACH*Cot_Angle	12	0	-10.1741	0.06023	27	-168.92	<.0001	0.05
ACH*Cot_Angle	12	30	-10.3492	0.06023	27	-171.83	<.0001	0.05
ACH*Cot_Angle	12	60	-10.2802	0.06023	27	-170.68	<.0001	0.05

Least Squares Means

Effect	ACH	Cot_Angle	Lower	Upper
ACH*Cot_Angle	0	0	-9.0197	-8.7726
ACH*Cot_Angle	0	30	-9.6323	-9.3852
ACH*Cot_Angle	0	60	-9.6730	-9.4259
ACH*Cot_Angle	5	0	-9.6060	-9.3589
ACH*Cot_Angle	5	30	-9.6263	-9.3792
ACH*Cot_Angle	5	60	-9.6691	-9.4220
ACH*Cot_Angle	12	0	-10.2977	-10.0505
ACH*Cot_Angle	12	30	-10.4728	-10.2257
ACH*Cot_Angle	12	60	-10.4038	-10.1566

Differences of Least Squares Means

Effect	ACH	Cot_Angle	ACH	Cot_Angle	Adjustment	Adj P	Alpha	Lower	Upper
ACH*Cot_Angle	0	0	0	30	Tukey	<.0001	0.05	0.4378	0.7873
ACH*Cot_Angle	0	0	0	60	Tukey	<.0001	0.05	0.4785	0.8281
ACH*Cot_Angle	0	0	5	0	Tukey	<.0001	0.05	0.4115	0.7611
ACH*Cot_Angle	0	0	5	30	Tukey	<.0001	0.05	0.4318	0.7813
ACH*Cot_Angle	0	0	5	60	Tukey	<.0001	0.05	0.4746	0.8241
ACH*Cot_Angle	0	0	12	0	Tukey	<.0001	0.05	1.1032	1.4527
ACH*Cot_Angle	0	0	12	30	Tukey	<.0001	0.05	1.2783	1.6279
ACH*Cot_Angle	0	0	12	60	Tukey	<.0001	0.05	1.2092	1.5588
ACH*Cot_Angle	0	30	0	60	Tukey	0.9999	0.05	-0.1341	0.2155
ACH*Cot_Angle	0	30	5	0	Tukey	1.0000	0.05	-0.2010	0.1485
ACH*Cot_Angle	0	30	5	30	Tukey	1.0000	0.05	-0.1808	0.1688
ACH*Cot_Angle	0	30	5	60	Tukey	1.0000	0.05	-0.1380	0.2116
ACH*Cot_Angle	0	30	12	0	Tukey	<.0001	0.05	0.4906	0.8402
ACH*Cot_Angle	0	30	12	30	Tukey	<.0001	0.05	0.6657	1.0153
ACH*Cot_Angle	0	30	12	60	Tukey	<.0001	0.05	0.5967	0.9462
ACH*Cot_Angle	0	60	5	0	Tukey	0.9964	0.05	-0.2418	0.1078
ACH*Cot_Angle	0	60	5	30	Tukey	0.9997	0.05	-0.2215	0.1281
ACH*Cot_Angle	0	60	5	60	Tukey	1.0000	0.05	-0.1787	0.1709
ACH*Cot_Angle	0	60	12	0	Tukey	<.0001	0.05	0.4499	0.7994
ACH*Cot_Angle	0	60	12	30	Tukey	<.0001	0.05	0.6250	0.9746
ACH*Cot_Angle	0	60	12	60	Tukey	<.0001	0.05	0.5560	0.9055
ACH*Cot_Angle	5	0	5	30	Tukey	1.0000	0.05	-0.1545	0.1950
ACH*Cot_Angle	5	0	5	60	Tukey	0.9976	0.05	-0.1117	0.2378
ACH*Cot_Angle	5	0	12	0	Tukey	<.0001	0.05	0.5169	0.8664
ACH*Cot_Angle	5	0	12	30	Tukey	<.0001	0.05	0.6920	1.0415
ACH*Cot_Angle	5	0	12	60	Tukey	<.0001	0.05	0.6229	0.9725
ACH*Cot_Angle	5	30	5	60	Tukey	0.9999	0.05	-0.1320	0.2176
ACH*Cot_Angle	5	30	12	0	Tukey	<.0001	0.05	0.4966	0.8462
ACH*Cot_Angle	5	30	12	30	Tukey	<.0001	0.05	0.6717	1.0213
ACH*Cot_Angle	5	30	12	60	Tukey	<.0001	0.05	0.6027	0.9522
ACH*Cot_Angle	5	60	12	0	Tukey	<.0001	0.05	0.4538	0.8034
ACH*Cot_Angle	5	60	12	30	Tukey	<.0001	0.05	0.6289	0.9785
ACH*Cot_Angle	5	60	12	60	Tukey	<.0001	0.05	0.5599	0.9094
ACH*Cot_Angle	12	0	12	30	Tukey	0.5210	0.05	0.000351	0.3499
ACH*Cot_Angle	12	0	12	60	Tukey	0.9384	0.05	-0.06871	0.2808
ACH*Cot_Angle	12	30	12	60	Tukey	0.9955	0.05	-0.2438	0.1057

Differences of Least Squares Means

Effect	ACH	Cot_Angle	ACH	Cot_Angle	Adj Lower	Adj Upper
ACH*Cot_Angle	0	0	0	30	0.3260	0.8992
ACH*Cot_Angle	0	0	0	60	0.3667	0.9399
ACH*Cot_Angle	0	0	5	0	0.2997	0.8729
ACH*Cot_Angle	0	0	5	30	0.3200	0.8932
ACH*Cot_Angle	0	0	5	60	0.3628	0.9360
ACH*Cot_Angle	0	0	12	0	0.9914	1.5646
ACH*Cot_Angle	0	0	12	30	1.1665	1.7397
ACH*Cot_Angle	0	0	12	60	1.0974	1.6706
ACH*Cot_Angle	0	30	0	60	-0.2459	0.3273
ACH*Cot_Angle	0	30	5	0	-0.3129	0.2603
ACH*Cot_Angle	0	30	5	30	-0.2926	0.2806
ACH*Cot_Angle	0	30	5	60	-0.2498	0.3234
ACH*Cot_Angle	0	30	12	0	0.3788	0.9520
ACH*Cot_Angle	0	30	12	30	0.5539	1.1271
ACH*Cot_Angle	0	30	12	60	0.4848	1.0580
ACH*Cot_Angle	0	60	5	0	-0.3536	0.2196
ACH*Cot_Angle	0	60	5	30	-0.3333	0.2399
ACH*Cot_Angle	0	60	5	60	-0.2905	0.2827
ACH*Cot_Angle	0	60	12	0	0.3381	0.9113
ACH*Cot_Angle	0	60	12	30	0.5132	1.0864
ACH*Cot_Angle	0	60	12	60	0.4441	1.0173
ACH*Cot_Angle	5	0	5	30	-0.2663	0.3069
ACH*Cot_Angle	5	0	5	60	-0.2235	0.3497
ACH*Cot_Angle	5	0	12	0	0.4050	0.9783
ACH*Cot_Angle	5	0	12	30	0.5802	1.1534
ACH*Cot_Angle	5	0	12	60	0.5111	1.0843
ACH*Cot_Angle	5	30	5	60	-0.2438	0.3294
ACH*Cot_Angle	5	30	12	0	0.3848	0.9580
ACH*Cot_Angle	5	30	12	30	0.5599	1.1331
ACH*Cot_Angle	5	30	12	60	0.4908	1.0640
ACH*Cot_Angle	5	60	12	0	0.3420	0.9152
ACH*Cot_Angle	5	60	12	30	0.5171	1.0903
ACH*Cot_Angle	5	60	12	60	0.4480	1.0212
ACH*Cot_Angle	12	0	12	30	-0.1115	0.4617
ACH*Cot_Angle	12	0	12	60	-0.1805	0.3927
ACH*Cot_Angle	12	30	12	60	-0.3557	0.2175

Results for Position 3:

The Mixed Procedure

Model Information

Data Set	WORK.NEW
Dependent Variable	logConc
Covariance Structure	Diagonal
Estimation Method	REML
Residual Variance Method	Profile
Fixed Effects SE Method	Model-Based
Degrees of Freedom Method	Residual

Class Level Information

Class	Levels	Values
ACH	3	0 5 12
Cot_Angle	2	0 30
Position	1	3

Dimensions

Covariance Parameters	1
Columns in X	12
Columns in Z	0
Subjects	1
Max Obs per Subject	24

Number of Observations

Number of Observations Read	24
Number of Observations Used	24
Number of Observations Not Used	0

Covariance Parameter Estimates

Cov Parm	Estimate
Residual	0.01771

Fit Statistics

-2 Res Log Likelihood	-13.2
AIC (Smaller is Better)	-11.2

AICC (Smaller is Better)	-11.0
BIC (Smaller is Better)	-10.3

The Mixed Procedure

Type 3 Tests of Fixed Effects

Effect	Num DF	Den DF	F Value	Pr > F
Cot_Angle	1	18	0.19	0.6661
ACH	2	18	155.26	<.0001
ACH*Cot_Angle	2	18	0.80	0.4656

Least Squares Means

Effect	ACH	Cot_Angle	Estimate	Standard Error	DF	t Value	Pr > |t|	Alpha
ACH*Cot_Angle	0	0	-9.2490	0.06654	18	-139.00	<.0001	0.05
ACH*Cot_Angle	0	30	-9.1285	0.06654	18	-137.19	<.0001	0.05
ACH*Cot_Angle	5	0	-9.5616	0.06654	18	-143.70	<.0001	0.05
ACH*Cot_Angle	5	30	-9.5786	0.06654	18	-143.96	<.0001	0.05
ACH*Cot_Angle	12	0	-10.3237	0.06654	18	-155.15	<.0001	0.05
ACH*Cot_Angle	12	30	-10.3556	0.06654	18	-155.63	<.0001	0.05

Least Squares Means

Effect	ACH	Cot_Angle	Lower	Upper
ACH*Cot_Angle	0	0	-9.3888	-9.1092
ACH*Cot_Angle	0	30	-9.2683	-8.9887
ACH*Cot_Angle	5	0	-9.7014	-9.4218
ACH*Cot_Angle	5	30	-9.7184	-9.4388
ACH*Cot_Angle	12	0	-10.4634	-10.1839
ACH*Cot_Angle	12	30	-10.4954	-10.2158

The Mixed Procedure

Differences of Least Squares Means

Effect	ACH	Cot_Angle	ACH	Cot_Angle	Adjustment	Adj P	Alpha	Lower	Upper
ACH*Cot_Angle	0	0	0	30	Tukey	0.7914	0.05	-0.3182	0.07718
ACH*Cot_Angle	0	0	5	0	Tukey	0.0375	0.05	0.1149	0.5103
ACH*Cot_Angle	0	0	5	30	Tukey	0.0260	0.05	0.1320	0.5274
ACH*Cot_Angle	0	0	12	0	Tukey	<.0001	0.05	0.8770	1.2724
ACH*Cot_Angle	0	0	12	30	Tukey	<.0001	0.05	0.9089	1.3043
ACH*Cot_Angle	0	30	5	0	Tukey	0.0026	0.05	0.2354	0.6308
ACH*Cot_Angle	0	30	5	30	Tukey	0.0018	0.05	0.2525	0.6479
ACH*Cot_Angle	0	30	12	0	Tukey	<.0001	0.05	0.9975	1.3929
ACH*Cot_Angle	0	30	12	30	Tukey	<.0001	0.05	1.0294	1.4248
ACH*Cot_Angle	5	0	5	30	Tukey	1.0000	0.05	-0.1806	0.2148
ACH*Cot_Angle	5	0	12	0	Tukey	<.0001	0.05	0.5644	0.9598
ACH*Cot_Angle	5	0	12	30	Tukey	<.0001	0.05	0.5963	0.9917
ACH*Cot_Angle	5	30	12	0	Tukey	<.0001	0.05	0.5473	0.9427
ACH*Cot_Angle	5	30	12	30	Tukey	<.0001	0.05	0.5793	0.9746
ACH*Cot_Angle	12	0	12	30	Tukey	0.9993	0.05	-0.1658	0.2296

Differences of Least Squares Means

Effect	ACH	Cot_Angle	ACH	Cot_Angle	Adj Lower	Adj Upper
ACH*Cot_Angle	0	0	0	30	-0.4196	0.1785
ACH*Cot_Angle	0	0	5	0	0.01354	0.6116
ACH*Cot_Angle	0	0	5	30	0.03061	0.6287
ACH*Cot_Angle	0	0	12	0	0.7756	1.3737
ACH*Cot_Angle	0	0	12	30	0.8076	1.4057
ACH*Cot_Angle	0	30	5	0	0.1341	0.7322
ACH*Cot_Angle	0	30	5	30	0.1511	0.7492
ACH*Cot_Angle	0	30	12	0	0.8961	1.4942
ACH*Cot_Angle	0	30	12	30	0.9281	1.5262
ACH*Cot_Angle	5	0	5	30	-0.2820	0.3161
ACH*Cot_Angle	5	0	12	0	0.4630	1.0611
ACH*Cot_Angle	5	0	12	30	0.4950	1.0931
ACH*Cot_Angle	5	30	12	0	0.4460	1.0441
ACH*Cot_Angle	5	30	12	30	0.4779	1.0760
ACH*Cot_Angle	12	0	12	30	-0.2671	0.3310

Results for Position 4:

The Mixed Procedure
Model Information

Data Set	WORK.NEW
Dependent Variable	logConc
Covariance Structure	Diagonal
Estimation Method	REML
Residual Variance Method	Profile
Fixed Effects SE Method	Model-Based
Degrees of Freedom Method	Residual

Class Level Information

Class	Levels	Values
ACH	3	0 5 12
Cot_Angle	3	0 30 60
Position	1	4

Dimensions

Covariance Parameters	1
Columns in X	16
Columns in Z	0
Subjects	1
Max Obs per Subject	36

Number of Observations

Number of Observations Read	36
Number of Observations Used	36
Number of Observations Not Used	0

Covariance Parameter Estimates

Cov Parm	Estimate
Residual	0.009615

Fit Statistics

-2 Res Log Likelihood	-36.3
AIC (Smaller is Better)	-34.3
AICC (Smaller is Better)	-34.1
BIC (Smaller is Better)	-33.0

Type 3 Tests of Fixed Effects

Effect	Num DF	Den DF	F Value	Pr > F
Cot_Angle	2	27	11.29	0.0003
ACH	2	27	476.82	<.0001
ACH*Cot_Angle	4	27	9.62	<.0001

Least Squares Means

Effect	ACH	Cot_Angle	Estimate	Standard Error	DF	t Value	Pr > |t|	Alpha
ACH*Cot_Angle	0	0	-9.0971	0.04903	27	-185.55	<.0001	0.05
ACH*Cot_Angle	0	30	-8.8588	0.04903	27	-180.69	<.0001	0.05
ACH*Cot_Angle	0	60	-9.3775	0.04903	27	-191.27	<.0001	0.05
ACH*Cot_Angle	5	0	-9.5796	0.04903	27	-195.39	<.0001	0.05
ACH*Cot_Angle	5	30	-9.6116	0.04903	27	-196.05	<.0001	0.05
ACH*Cot_Angle	5	60	-9.7144	0.04903	27	-198.14	<.0001	0.05
ACH*Cot_Angle	12	0	-10.3409	0.04903	27	-210.92	<.0001	0.05
ACH*Cot_Angle	12	30	-10.3759	0.04903	27	-211.64	<.0001	0.05
ACH*Cot_Angle	12	60	-10.3115	0.04903	27	-210.32	<.0001	0.05

Least Squares Means

Effect	ACH	Cot_Angle	Lower	Upper
ACH*Cot_Angle	0	0	-9.1977	-8.9965
ACH*Cot_Angle	0	30	-8.9594	-8.7582
ACH*Cot_Angle	0	60	-9.4781	-9.2769
ACH*Cot_Angle	5	0	-9.6802	-9.4790
ACH*Cot_Angle	5	30	-9.7122	-9.5110
ACH*Cot_Angle	5	60	-9.8150	-9.6138
ACH*Cot_Angle	12	0	-10.4415	-10.2403
ACH*Cot_Angle	12	30	-10.4764	-10.2753
ACH*Cot_Angle	12	60	-10.4121	-10.2109

Differences of Least Squares Means

Effect	ACH	Cot_Angle	ACH	Cot_Angle	Adjustment	Adj P	Alpha	Lower	Upper
ACH*Cot_Angle	0	0	0	30	Tukey	0.0424	0.05	-0.3806	-0.09608
ACH*Cot_Angle	0	0	0	60	Tukey	0.0101	0.05	0.1381	0.4226
ACH*Cot_Angle	0	0	5	0	Tukey	<.0001	0.05	0.3402	0.6247
ACH*Cot_Angle	0	0	5	30	Tukey	<.0001	0.05	0.3722	0.6568
ACH*Cot_Angle	0	0	5	60	Tukey	<.0001	0.05	0.4750	0.7595
ACH*Cot_Angle	0	0	12	0	Tukey	<.0001	0.05	1.1015	1.3860
ACH*Cot_Angle	0	0	12	30	Tukey	<.0001	0.05	1.1365	1.4210
ACH*Cot_Angle	0	0	12	60	Tukey	<.0001	0.05	1.0722	1.3567
ACH*Cot_Angle	0	30	0	60	Tukey	<.0001	0.05	0.3765	0.6610
ACH*Cot_Angle	0	30	5	0	Tukey	<.0001	0.05	0.5785	0.8631
ACH*Cot_Angle	0	30	5	30	Tukey	<.0001	0.05	0.6106	0.8951
ACH*Cot_Angle	0	30	5	60	Tukey	<.0001	0.05	0.7133	0.9979
ACH*Cot_Angle	0	30	12	0	Tukey	<.0001	0.05	1.3399	1.6244
ACH*Cot_Angle	0	30	12	30	Tukey	<.0001	0.05	1.3748	1.6593
ACH*Cot_Angle	0	30	12	60	Tukey	<.0001	0.05	1.3105	1.5950
ACH*Cot_Angle	0	60	5	0	Tukey	0.1295	0.05	0.05980	0.3443
ACH*Cot_Angle	0	60	5	30	Tukey	0.0487	0.05	0.09185	0.3764
ACH*Cot_Angle	0	60	5	60	Tukey	0.0013	0.05	0.1946	0.4791
ACH*Cot_Angle	0	60	12	0	Tukey	<.0001	0.05	0.8211	1.1057
ACH*Cot_Angle	0	60	12	30	Tukey	<.0001	0.05	0.8561	1.1406
ACH*Cot_Angle	0	60	12	60	Tukey	<.0001	0.05	0.7918	1.0763
ACH*Cot_Angle	5	0	5	30	Tukey	0.9999	0.05	-0.1102	0.1743
ACH*Cot_Angle	5	0	5	60	Tukey	0.5914	0.05	-0.00745	0.2771
ACH*Cot_Angle	5	0	12	0	Tukey	<.0001	0.05	0.6191	0.9036
ACH*Cot_Angle	5	0	12	30	Tukey	<.0001	0.05	0.6540	0.9385
ACH*Cot_Angle	5	0	12	60	Tukey	<.0001	0.05	0.5897	0.8742
ACH*Cot_Angle	5	30	5	60	Tukey	0.8540	0.05	-0.03950	0.2450
ACH*Cot_Angle	5	30	12	0	Tukey	<.0001	0.05	0.5870	0.8715
ACH*Cot_Angle	5	30	12	30	Tukey	<.0001	0.05	0.6220	0.9065
ACH*Cot_Angle	5	30	12	60	Tukey	<.0001	0.05	0.5577	0.8422
ACH*Cot_Angle	5	60	12	0	Tukey	<.0001	0.05	0.4843	0.7688
ACH*Cot_Angle	5	60	12	30	Tukey	<.0001	0.05	0.5192	0.8037
ACH*Cot_Angle	5	60	12	60	Tukey	<.0001	0.05	0.4549	0.7394
ACH*Cot_Angle	12	0	12	30	Tukey	0.9999	0.05	-0.1073	0.1772
ACH*Cot_Angle	12	0	12	60	Tukey	1.0000	0.05	-0.1716	0.1129
ACH*Cot_Angle	12	30	12	60	Tukey	0.9892	0.05	-0.2066	0.07795

Differences of Least Squares Means

Effect	ACH	Cot_Angle	ACH	Cot_Angle	Adj Lower	Adj Upper
ACH*Cot_Angle	0	0	0	30	-0.4716	-0.00505
ACH*Cot_Angle	0	0	0	60	0.04709	0.5137
ACH*Cot_Angle	0	0	5	0	0.2492	0.7157
ACH*Cot_Angle	0	0	5	30	0.2812	0.7478
ACH*Cot_Angle	0	0	5	60	0.3840	0.8505
ACH*Cot_Angle	0	0	12	0	1.0105	1.4771
ACH*Cot_Angle	0	0	12	30	1.0454	1.5120
ACH*Cot_Angle	0	0	12	60	0.9811	1.4477
ACH*Cot_Angle	0	30	0	60	0.2854	0.7520
ACH*Cot_Angle	0	30	5	0	0.4875	0.9541
ACH*Cot_Angle	0	30	5	30	0.5196	0.9861
ACH*Cot_Angle	0	30	5	60	0.6223	1.0889
ACH*Cot_Angle	0	30	12	0	1.2488	1.7154
ACH*Cot_Angle	0	30	12	30	1.2838	1.7504
ACH*Cot_Angle	0	30	12	60	1.2195	1.6861
ACH*Cot_Angle	0	60	5	0	-0.03123	0.4354
ACH*Cot_Angle	0	60	5	30	0.000825	0.4674
ACH*Cot_Angle	0	60	5	60	0.1036	0.5702
ACH*Cot_Angle	0	60	12	0	0.7301	1.1967
ACH*Cot_Angle	0	60	12	30	0.7651	1.2316
ACH*Cot_Angle	0	60	12	60	0.7007	1.1673
ACH*Cot_Angle	5	0	5	30	-0.2012	0.2653
ACH*Cot_Angle	5	0	5	60	-0.09848	0.3681
ACH*Cot_Angle	5	0	12	0	0.5280	0.9946
ACH*Cot_Angle	5	0	12	30	0.5630	1.0296
ACH*Cot_Angle	5	0	12	60	0.4987	0.9653
ACH*Cot_Angle	5	30	5	60	-0.1305	0.3360
ACH*Cot_Angle	5	30	12	0	0.4960	0.9626
ACH*Cot_Angle	5	30	12	30	0.5309	0.9975
ACH*Cot_Angle	5	30	12	60	0.4666	0.9332
ACH*Cot_Angle	5	60	12	0	0.3932	0.8598
ACH*Cot_Angle	5	60	12	30	0.4282	0.8948
ACH*Cot_Angle	5	60	12	60	0.3639	0.8305
ACH*Cot_Angle	12	0	12	30	-0.1983	0.2682
ACH*Cot_Angle	12	0	12	60	-0.2627	0.2039
ACH*Cot_Angle	12	30	12	60	-0.2976	0.1690

Results for Position 5 are not displayed because there is only one level of cot angle (60°) for that position.